AD-A056 642 DEFENCE RESEARCH ESTABLISHMENT VALCARTIER (QUEBEC) F/G 20/5
AVERAGE IRRADIANCE AND IRRADIANCE VARIANCE OF LASER BEAMS IN TU--ETC(U)
MAY 78 L R BISSONNETTE

UNCLASSIFIED DREV-R-4104/78 NL

| OF |
AD
A056642

END
DATE
FILMED
9-78
DDC

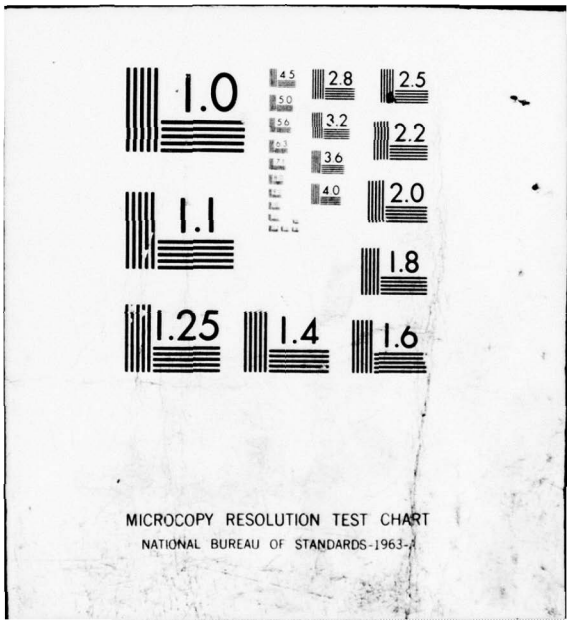
1.0
1.1
1.25
1.4
1.6
1.8
2.0
2.2
2.5
2.8
3.2
3.6
4.0
4.5
5.0
5.6
6.3
MICROCOPY RESOLUTION TEST CHART
NATIONAL BUREAU OF STANDARDS-1963-A

UNCLASSIFIED

CRDV RAPPORT 4104/78
DOSSIER: 3621T-005
MAI 1978

LEVEL II

DREV REPORT 4104/78
FILE: 3621T-005
MAY 1978

(3)

AVERAGE IRRADIANCE AND IRRADIANCE VARIANCE OF LASER BEAMS IN TURBULENT MEDIA

L.R. Bissonnette

Centre de Recherches pour la Défense
Defence Research Establishment
Valcartier, Québec

BUREAU - RECHERCHE ET DÉVELOPPEMENT
MINISTÈRE DE LA DÉFENSE NATIONALE
CANADA

RESEARCH AND DEVELOPMENT BRANCH
DEPARTMENT OF NATIONAL DEFENCE
CANADA

NON CLASSIFIÉ

(6) AVERAGE IRRADIANCE AND IRRADIANCE VARIANCE OF LASER BEAMS IN TURBULENT MEDIA,

by

(10) L.R. Bissonnette

(11) MAY 78

(12) 63p.

CENTRE DE RECHERCHES POUR LA DEFENSE

DEFENCE RESEARCH ESTABLISHMENT

VALCARTIER

Tel: (418) 844-4271

Québec, Canada

May/mai 1978

NON CLASSIFIE

RESUME

On a mis au point un modèle semi-empirique de la propagation de faisceaux laser en milieux turbulents sous la forme d'un système fermé d'équations aux dérivées partielles du second ordre pour les moments statistiques du premier et du second ordres de l'amplitude de l'onde lumineuse. Ces équations sont linéaires, ne contiennent que des coefficients algébriques et sont uniformément valides à toutes les distances de propagation. On montre que l'hypothèse de la fonction de probabilité normale de l'amplitude complexe de l'onde est compatible avec l'équation d'onde stochastique. Cette hypothèse est utilisée pour écrire la variance de l'intensité en fonction des moments d'ordres un et deux de l'amplitude. Les profils de l'intensité moyenne et de la variance de l'intensité des faisceaux laser sont facilement et rapidement calculés au moyen d'une méthode numérique aux différences finies. Les résultats sont en excellent accord avec des mesures expérimentales prises dans l'atmosphère et en milieu de simulation. (NC)

ABSTRACT

A semi-empirical model of laser beam propagation in turbulence is written in the form of a closed set of second-order partial differential equations for the first- and second-order amplitude moments. The equations are linear, contain only algebraic coefficients, and are uniformly valid over the complete propagation range. The hypothesis of normal probability distribution of the complex wave amplitude is shown to be consistent with the stochastic wave equation, and is used to obtain the irradiance variance in terms of the first- and second-order amplitude moments. Solutions for average irradiance and irradiance variance profiles of laser beams are easily and quickly calculated by a numerical finite difference method. Predictions agree very well with experimental data in the atmosphere and in a simulation medium. (U)

TABLE OF CONTENTS

1.0 INTRODUCTION

Atmospheric propagation of laser beams is affected by turbulence. The refractive index fluctuations cause the beam to scintillate or break up in several random patches, to lose its spatial coherence, to wander about its axis, and to spread out. These behaviours are detrimental to military applications both at low and high power levels. Some adverse effects are: a reduction of signal-to-noise ratio in detection, ranging and communication, a loss of average power density on targets, a lowering of breakdown threshold owing to the presence of intense peaks relative to average irradiance, etc. Consequently, the modelling of optical and infrared wave propagation in turbulence is important for the design and the assessment of military laser systems.

The analytical Rytov method, fully documented in Refs. 1 and 2, gives excellent results in the weak scintillation limit, i.e. at small propagation distance and/or turbulence strength. However, it is well-known that the Rytov method fails when irradiance fluctuations reach a certain level: theory predicts an unlimited increase of irradiance variance whereas experiments definitely show saturation. Many recent models deal with this problem and predict, with variable degrees of accuracy, the phenomenon of saturation. A first approach, known as the renormalization technique, is described in Ref. 2. For example, de Wolf (Refs. 3-6) used it to predict saturation of the irradiance variance. A second approach consists in solving a differential equation for the

fourth-order statistical moment of the complex electric field closed by local application of the method of small perturbation. This method originated in the USSR and is reviewed in Ref. 7. Examples of solutions showing saturation are given in Refs. 8 to 11. A third approach is based on the extension of the Huygens-Fresnel principle to turbulent media (Ref. 12). Saturation results derived from various methods of application of this principle are described in Refs. 13 to 17. Finally, Sancer and Varvatsis (Ref. 18) have proposed an independent model which was among the first to show saturation of the irradiance variance. Although their solution was relatively simple and in reasonable agreement with data, the constitutive hypotheses were poorly justified (Ref. 19) and the method was unfortunately not revised nor pursued any further.

It is not our purpose here to discuss the merit of each of the theoretical models listed in the preceding paragraph. However, one characteristic they all share is that it is difficult and lengthy to compute numerical results from the proposed solutions. One has either to solve a four-fold partial differential equation or to evaluate multiple integrals at each spatial point. Moreover, the predicted irradiance variance is generally too small in the strong scintillation region. Here, we propose a semi-empirical model in the form of linear second-order partial differential equations from which the average irradiance and the irradiance variance profiles can be easily and quickly calculated for any beam geometry.

This work was performed at DREV between November 1976 and October 1977 under PCN 21T05, Propagation of Laser Beams.

2.0 THEORETICAL BACKGROUND

2.1 Equations for the Instantaneous Field

The basic model for optical and infrared wave propagation is described in Ref. 20. We shall briefly review the hypotheses and the derivation steps.

The propagation medium is assumed to have a constant relative magnetic permeability μ and a randomly fluctuating relative dielectric constant ε. Without loss of generality, we neglect absorption so that $\varepsilon\mu = N^2$, where N is the refractive index. It is known from observations that the fluctuating part of N is much smaller than its average or unperturbed value n_o and, therefore, polarization can be neglected. Under these conditions the electric field vector $\underset{\sim}{E}$ of the optical wave can be treated as a scalar E. In the present model, E is written as follows:

$$E = A \exp [ik(\phi+z) - i\omega t] \quad , \tag{1}$$

where A is a complex wave amplitude; $k\phi$, a phase function to be determined; z, the propagation distance; $k = n_o\omega/c$, the wave number; ω, the angular frequency of the assumed monochromatic source; c, the speed of light in

free space; t, the time; and $i = \sqrt{-1}$. Upon substituting relation (1) for E in the scalar wave equation for the electric field derived from Maxwell's equations (Ref. 21) and making the paraxial approximation valid for propagation in atmospheric turbulence, we obtain after separation:

$$\left(\frac{\partial}{\partial z} + \underset{\sim}{V}\right)\underset{\sim}{V} = \underset{\sim}{\nabla}(N-n_o)/n_o \quad , \tag{2}$$

$$\left(\frac{\partial}{\partial z} + \underset{\sim}{V}.\underset{\sim}{\nabla}\right)A + \tfrac{1}{2}A\underset{\sim}{\nabla}.\underset{\sim}{V} - \frac{i}{2k}\,\underset{\sim}{\nabla}^2 A = 0 \quad . \tag{3}$$

The vector $\underset{\sim}{V}$ is defined as follows:

$$\underset{\sim}{V} = \underset{\sim}{\nabla}\phi \quad , \tag{4}$$

and $\underset{\sim}{\nabla}$ is the gradient operator in the plane transverse to the direction of propagation.

Equation (2) is the paraxial form of the eikonal equation. Hence, $\underset{\sim}{V}$ is the vector angle made by the local instantaneous geometrical rays and, from equation (1), it follows that A is the complex wave amplitude defined on the geometrical phase front. The operator $\left(\frac{\partial}{\partial z} + \underset{\sim}{V}.\underset{\sim}{\nabla}\right)$ indicates differentiation along a ray. The term $\frac{1}{2}A\underset{\sim}{\nabla}.\underset{\sim}{V}$ represents the geometrical effects on the complex amplitude A of the converging and diverging rays and $\frac{i}{2k}\,\underset{\sim}{\nabla}^2 A$ is the diffractional contribution which tends to "diffuse" A. Neglecting the latter term on the grounds that k is large constitutes the geometrical optics approximation.

Since the refractive index N is a random function, equations (2) and (3) are stochastic equations. There is no known general method for solving the random functions $\underset{\sim}{V}$ and A. Even if that could be achieved, it would yield much more information than required in practice. Here, the stochastic equations (2) and (3) are used to obtain differential equations for those statistical moments of $\underset{\sim}{V}$ and A that are of interest.

2.2 Equations for the First- and Second-Order Moments of the Complex Wave Amplitude

We confine ourselves to the first- and second-order moments of the complex wave amplitude which lend themselves to straightforward and meaningful physical interpretations. More sophisticated developments involving covariances and higher-order moments are contingent to the successful verification of this simpler model.

The random functions are written as sums of an average and a fluctuating part, i.e.:

$$N = n_o + n \quad ; \quad \langle n \rangle = 0 \quad , \tag{5}$$

$$\underset{\sim}{V} = \langle \underset{\sim}{V} \rangle + \underset{\sim}{v} \quad ; \quad \langle \underset{\sim}{v} \rangle = 0 \quad , \tag{6}$$

$$A = \langle A \rangle + a \quad ; \quad \langle a \rangle = 0 \quad , \tag{7}$$

where the angular brackets denote ensemble averages. The equations for the moments are obtained by taking the ensemble average of the stochastic equations for $\underset{\sim}{V}$, A, AA and AA* derived from governing equations (2) and (3). We find (Ref. 20):

$$\left(\frac{\partial}{\partial z} + \langle \underset{\sim}{V} \rangle . \underset{\sim}{\nabla}\right) \langle \underset{\sim}{V} \rangle = - \tfrac{1}{2} \underset{\sim}{\nabla} \langle \underset{\sim}{v} . \underset{\sim}{v} \rangle \quad , \tag{8}$$

$$\left(\frac{\partial}{\partial z} + \langle \underset{\sim}{V} \rangle . \underset{\sim}{\nabla}\right) \langle A \rangle + \tfrac{1}{2} \langle A \rangle \underset{\sim}{\nabla} . \langle \underset{\sim}{V} \rangle - \frac{i}{2k} \underset{\sim}{\nabla}^2 \langle A \rangle$$

$$= - \underset{\sim}{\nabla} . \langle \underset{\sim}{v} a \rangle + \tfrac{1}{2} \langle a \underset{\sim}{\nabla} . \underset{\sim}{v} \rangle \quad , \tag{9}$$

$$\left(\frac{\partial}{\partial z} + \langle \underset{\sim}{V} \rangle . \underset{\sim}{\nabla}\right) \langle aa \rangle + \langle aa \rangle \underset{\sim}{\nabla} . \langle \underset{\sim}{V} \rangle - \frac{i}{2k} \underset{\sim}{\nabla}^2 \langle aa \rangle + \frac{i}{k} \langle \underset{\sim}{\nabla} a . \underset{\sim}{\nabla} a \rangle$$

$$= - \underset{\sim}{\nabla} . \langle \underset{\sim}{v} aa \rangle - 2 \langle a \underset{\sim}{v} \rangle . \underset{\sim}{\nabla} \langle A \rangle - \langle A \rangle \langle a \underset{\sim}{\nabla} . \underset{\sim}{v} \rangle \quad , \tag{10}$$

$$\left(\frac{\partial}{\partial z} + \langle \underset{\sim}{V} \rangle . \underset{\sim}{\nabla}\right) \langle aa^* \rangle + \langle aa^* \rangle \underset{\sim}{\nabla} . \langle \underset{\sim}{V} \rangle - \frac{i}{2k} \underset{\sim}{\nabla} . [\langle a^* \underset{\sim}{\nabla} a \rangle - \langle a \underset{\sim}{\nabla} a^* \rangle]$$

$$= - \underset{\sim}{\nabla} . \langle \underset{\sim}{v} aa^* \rangle - \langle a \underset{\sim}{v} \rangle . \underset{\sim}{\nabla} \langle A \rangle^* - \langle a^* \underset{\sim}{v} \rangle . \underset{\sim}{\nabla} \langle A \rangle$$

$$- \tfrac{1}{2} \langle A \rangle^* \langle a \underset{\sim}{\nabla} . \underset{\sim}{v} \rangle - \tfrac{1}{2} \langle A \rangle \langle a^* \underset{\sim}{\nabla} . \underset{\sim}{v} \rangle \quad , \tag{11}$$

where the superscript * denotes a complex conjugate. The average irradiance is given by:

$$\langle I \rangle = \langle A \rangle \langle A \rangle^* + \langle aa^* \rangle \quad . \tag{12}$$

The physical interpretation of the mathematical terms in equations (8) to (11) is discussed in Ref. 20. We will simply identify here the principal mechanisms. The moments $\langle \underset{\sim}{v} a \rangle$, $\langle vaa^* \rangle$ and $\langle \underset{\sim}{v} aa \rangle$ are responsible for beam spreading and $\langle a \underset{\sim}{\nabla} . \underset{\sim}{v} \rangle$ for beam breakup or loss of coherence. The terms multiplied by (i/k) represent the explicit diffractionnal effects. Finally, the group of terms $[-\langle a \underset{\sim}{v} \rangle . \underset{\sim}{\nabla} \langle A \rangle^* - \tfrac{1}{2} \langle A \rangle^* \langle a \underset{\sim}{\nabla} . \underset{\sim}{v} \rangle + c.c.]$

models the production of turbulent irradiance, <aa*>, at the expense of coherent irradiance, <A><A>*.

2.3 Integral Solution for the Fluctuating Complex Amplitude

The average angle $\langle \underset{\sim}{V} \rangle$ is only weakly dependent on the variance of $\underset{\sim}{v}$. To show this, we rewrite equation (8):

$$\frac{\partial}{\partial z} \langle \underset{\sim}{V} \rangle + \tfrac{1}{2} \nabla_{\underset{\sim}{}} [\langle \underset{\sim}{V} \rangle . \langle \underset{\sim}{V} \rangle + \langle \underset{\sim}{v} . \underset{\sim}{v} \rangle] = 0 \quad . \tag{8}$$

To a factor of order unity, we have from small perturbation theory:

$$\langle \underset{\sim}{v} . \underset{\sim}{v} \rangle \simeq C_n^2 \, z/\ell_o^{1/3} \quad , \tag{13}$$

where C_n^2 is the index structure constant and ℓ_o, the inner scale of turbulence. Typically, for strong turbulence, i.e. $C_n^2 \simeq 2.5\text{x}10^{-14}$ $m^{-2/3}$, and $\ell_o \simeq 10^{-3}$ m, we have at 1 km $\langle \underset{\sim}{v} . \underset{\sim}{v} \rangle \simeq 2.5\text{x}10^{-10}$. By comparison, the average ray angle $\langle \underset{\sim}{V} \rangle$ is of the order of r_o/F where r_o is the characteristic radius of the beam and F, the focal length or the radius of the initial phase front curvature. For $r_o \simeq 0.1$ m and F = 1 km, we have $\langle \underset{\sim}{V} \rangle \langle \underset{\sim}{V} \rangle \simeq 10^{-8}$. Therefore, for practical applications, we can approximate:

$$\langle \underset{\sim}{V} \rangle . \langle \underset{\sim}{V} \rangle \; >> \; \langle \underset{\sim}{v} . \underset{\sim}{v} \rangle \quad , \tag{14}$$

and equation (8) becomes:

$$\frac{\partial}{\partial z} \langle \underset{\sim}{V} \rangle + \langle \underset{\sim}{V} \rangle . \underset{\sim}{\nabla} \langle \underset{\sim}{V} \rangle = 0 \quad . \tag{15}$$

For an initially spherical phase front with radius of curvature F, equation (15) has the solution:

$$\langle \underset{\sim}{V} \rangle = \frac{\underset{\sim}{r}}{(z - F)} \quad . \tag{16}$$

The equation for the fluctuating amplitude, a, is obtained by subtracting equation (9) from equation (3). We find, using equation (16):

$$\frac{\partial}{\partial z} a + \frac{\underset{\sim}{r}}{(z - F)} . \underset{\sim}{\nabla} a + \frac{a}{(z - F)} - \frac{i}{2k} \underset{\sim}{\nabla}^2 a = g(z, \underset{\sim}{r}) \tag{17}$$

where:

$$g(z, \underset{\sim}{r}) = - \underset{\sim}{v} . \underset{\sim}{\nabla} \langle A \rangle - \tfrac{1}{2} \langle A \rangle \underset{\sim}{\nabla} . \underset{\sim}{v}$$

$$- \underset{\sim}{\nabla} . [\underset{\sim}{v} a - \langle \underset{\sim}{v} a \rangle] + \tfrac{1}{2} [a \underset{\sim}{\nabla} . \underset{\sim}{v} - \langle a \underset{\sim}{\nabla} . \underset{\sim}{v} \rangle] \quad . \tag{18}$$

A solution to equation (17) with boundary conditions $a(0, \underset{\sim}{r}) = \lim_{|\underset{\sim}{r}| \to \infty} a(z, \underset{\sim}{r}) = 0$ is given by:

$$a(z, \underset{\sim}{r}) = \frac{ik}{2\pi} \int_0^z \frac{du}{(u - z)} \iint_{-\infty}^{\infty} d^2 \underset{\sim}{s} \exp \left[\frac{ik}{2(z - u)} \frac{(F - z)}{(F - u)} |\underset{\sim}{s} - \underset{\sim}{r}|^2 \right] g(u, \underset{\sim}{s}). \tag{19}$$

3.0 CLOSURE PROBLEM

The system of equations (9) to (11) for $\langle A \rangle$, $\langle aa \rangle$ and $\langle aa^* \rangle$ is mathematically unclosed insofar as it contains more unknowns than equations, namely the moments $\langle \underset{\sim}{v}a \rangle$, $\langle \underset{\sim}{v}aa \rangle$, $\langle \underset{\sim}{v}aa^* \rangle$ and $\langle a\underset{\sim}{\nabla}.\underset{\sim}{v} \rangle$. In principle, one could derive equations for these moments using a procedure analogous to that used in obtaining equations (9) to (11). However, one would quickly realize that this technique leads to equations involving still higher order and unknown moments. This is the classical closure problem which is always encountered in the treatment of statistical phenomena governed by nonlinear and/or quasi-linear stochastic equations as those given by equations (2) and (3). Of course, there is no exact method of solution for this problem since the complete mathematical model contains an infinite number of equations. Hence, workable models require closing the hierarchy of equations after moments of a given order. This can be accomplished only through approximations regarding the higher order moments for which the equations have been left out. In this report, we propose four relations to express $\langle \underset{\sim}{v}a \rangle$, $\langle \underset{\sim}{v}aa \rangle$, $\langle vaa^* \rangle$ and $\langle a\underset{\sim}{\nabla}.\underset{\sim}{v} \rangle$ as functions of $\langle A \rangle$, $\langle aa \rangle$ and $\langle aa^* \rangle$. Moreover, since we limit the analysis to variances only, we will need outside information to relate $\langle \underset{\sim}{\nabla}a.\underset{\sim}{\nabla}a \rangle$ to $\langle aa \rangle$.

3.1 Statistical Hypotheses

We summarize under this section the principal hypotheses that will be used to derive the constitutive relations for the unknown moments.

First, we assume that the fluctuating angle-of-arrival $\underset{\sim}{v}$ is statistically homogeneous and isotropic in the plane transverse to the main direction of propagation. This approximation follows from the hypothesis that the refractive index is statistically homogeneous and isotropic and from the paraxial approximation. Indeed, since the medium is homogeneous and isotropic and since the average ray angle $\langle \underset{\sim}{V} \rangle$ is small, the rays reaching a plane z have traversed nearly equivalent paths regardless of their point of arrival in that plane. Hence, the covariance function of $\underset{\sim}{v}$ should depend only on the relative positions of the observation points in plane z.

Second, we assume that the random amplitude, a, and angle-of-arrival, $\underset{\sim}{v}$, are only weakly correlated. Equation (19) shows that the fluctuating amplitude is the result of repeated interactions with the angle-of-arrival over the complete propagation path between 0 and z, and of diffraction scattering from turbulent regions off the optical axis. Hence, the local amplitude $a(z, \underset{\sim}{r})$ depends on many processes independent of the local angle-of-arrival $\underset{\sim}{v}(z, \underset{\sim}{r})$ and, therefore, the hypothesis of weak correlation appears very reasonable. More specifically, we assume that:

$$|\langle \underset{\sim}{v}_1 a_2 \rangle| \ll \langle \underset{\sim}{v} . \underset{\sim}{v} \rangle^{\frac{1}{2}} \langle I \rangle^{\frac{1}{2}} , \tag{20a}$$

$$|\langle \underset{\sim}{v}_1 \underset{\sim}{v}_2 a_2 \rangle| \ll \langle \underset{\sim}{v} . \underset{\sim}{v} \rangle \langle I \rangle^{\frac{1}{2}} , \tag{20b}$$

$$\langle \underset{\sim}{v}_1 \underset{\sim}{v}_2 a_1 a_2 \rangle \simeq \langle \underset{\sim}{v}_1 \underset{\sim}{v}_2 \rangle \langle a_1 a_2 \rangle + \{ |\text{terms}| \ll \langle \underset{\sim}{v}.\underset{\sim}{v} \rangle \langle I \rangle \} \quad , \tag{20c}$$

etc...

The subscripts 1 and 2 refer to the separation points of the covariance functions; where no subscripts are used, the midpoint between 1 and 2 is taken.

Finally, we assume that the covariance functions involving the fluctuating amplitude are quasi-homogeneous and quasi-isotropic in the transverse plane, i.e.:

$$\langle a(z_1,\underset{\sim}{r}_1)\, a(z_2,\underset{\sim}{r}_2) \rangle \simeq f_{aa}(z_1,z_2;\underset{\sim}{r}_1,\underset{\sim}{r}_2)\; g_{aa}(z_1,z_2;|\underset{\sim}{r}_1-\underset{\sim}{r}_2|) \quad , \tag{21a}$$

$$\langle a(z_1,\underset{\sim}{r}_1)\, a^*(z_2,\underset{\sim}{r}_2) \rangle \simeq f_{aa^*}(z_1,z_2;\underset{\sim}{r}_1,\underset{\sim}{r}_2)\; g_{aa^*}(z_1,z_2;|\underset{\sim}{r}_1-\underset{\sim}{r}_2|) \quad , \tag{21b}$$

where f_{aa} and f_{aa^*} are functions of both position vectors $\underset{\sim}{r}_1$ and $\underset{\sim}{r}_2$, and where g_{aa} and g_{aa^*} are functions of the magnitude of the vector difference only. More specifically, we set:

$$f_{aa} = \tfrac{1}{2} \langle a(z_1,\underset{\sim}{r}_1)\, a(z_1,\underset{\sim}{r}_1) \rangle + \tfrac{1}{2} \langle a(z_2,\underset{\sim}{r}_2)\, a(z_2,\underset{\sim}{r}_2) \rangle \quad , \tag{22a}$$

$$f_{aa^*} = \tfrac{1}{2} \langle a(z_1,\underset{\sim}{r}_1)\, a^*(z_1,\underset{\sim}{r}_1) \rangle + \tfrac{1}{2} \langle a(z_2,\underset{\sim}{r}_2)\, a^*(z_2,\underset{\sim}{r}_2) \rangle . \tag{22b}$$

Equations (21) and (22) constitute a standard approximation often made in the presence of average gradients.

3.2 Constitutive Relations

To obtain a relation for $\langle a\nabla.\underset{\sim}{v}\rangle$, we multiply equation (19) by $\nabla.\underset{\sim}{v}$ and then take the ensemble average. There results, inside the integral operator, an expression of the form:

$$\begin{aligned}\langle g(u,\underset{\sim}{s})\ \nabla.\underset{\sim}{v}(z,\underset{\sim}{r})\rangle \;=\; & -\left(\nabla_{\underset{\sim}{r}}.\langle \underset{\sim}{v}(z,\underset{\sim}{r})\ \underset{\sim}{v}(u,\underset{\sim}{s})\rangle\right).\nabla_{\underset{\sim}{s}}\ \langle A(u,\underset{\sim}{s})\rangle \\ & - \tfrac{1}{2}\left(\nabla_{\underset{\sim}{s}}\nabla_{\underset{\sim}{r}}:\langle \underset{\sim}{v}(z,\underset{\sim}{r})\ \underset{\sim}{v}(u,\underset{\sim}{s})\rangle\right)\ \langle A(u,\underset{\sim}{s})\rangle \\ & - \nabla_{\underset{\sim}{s}}\nabla_{\underset{\sim}{r}}:\langle \underset{\sim}{v}(z,\underset{\sim}{r})\ \underset{\sim}{v}(u,\underset{\sim}{s})\ a(u,\underset{\sim}{s})\rangle \\ & + \tfrac{1}{2}\left\langle\left(\nabla_{\underset{\sim}{r}}.\underset{\sim}{v}(z,\underset{\sim}{r})\right) a(u,\underset{\sim}{s})\ \nabla_{\underset{\sim}{s}}.\underset{\sim}{v}(u,\underset{\sim}{s})\right\rangle \quad . \end{aligned} \tag{23}$$

From our second hypothesis, we neglect the last two terms of equation (23), i.e. the third-order moments involving twice the angle-of-arrival $\underset{\sim}{v}$, as being much smaller than the first two terms which are of the order of the covariance of $\underset{\sim}{v}$. Hence, we have:

$$\begin{aligned}\langle g(u,\underset{\sim}{s})\ \nabla.\underset{\sim}{v}(z,\underset{\sim}{r})\rangle \;=\; & -\left(\nabla_{\underset{\sim}{r}}.\langle \underset{\sim}{v}(z,\underset{\sim}{r})\ \underset{\sim}{v}(u,\underset{\sim}{s})\rangle\right).\nabla_{\underset{\sim}{s}}\langle A(u,\underset{\sim}{s})\rangle \\ & - \tfrac{1}{2}\left(\nabla_{\underset{\sim}{s}}\nabla_{\underset{\sim}{r}}:\langle \underset{\sim}{v}(z,\underset{\sim}{r})\ \underset{\sim}{v}(u,\underset{\sim}{s})\rangle\right)\langle A(u,\underset{\sim}{s})\rangle \quad . \end{aligned} \tag{24}$$

It is convenient at this point to make the following change of variables:

$$(\underset{\sim}{r}, \underset{\sim}{s}) \rightarrow (\underset{\sim}{r}, \underset{\sim}{\rho}) \quad , \tag{25a}$$

with:

$$\underset{\sim}{\rho} = \underset{\sim}{s} - \underset{\sim}{r} \quad , \tag{25b}$$

from where it follows:

$$\underset{\sim}{\nabla}_r \rightarrow \underset{\sim}{\nabla}_r - \underset{\sim}{\nabla}_\rho \quad , \tag{25c}$$

$$\underset{\sim}{\nabla}_s \rightarrow \underset{\sim}{\nabla}_\rho \quad . \tag{25d}$$

Also, from the hypothesis that $\underset{\sim}{v}$ is statistically homogeneous and isotropic in the transverse plane and the theory of isotropic tensors (Ref. 22), we have:

$$\langle \underset{\sim}{v}(z,\underset{\sim}{r})\ \underset{\sim}{v}(u,\underset{\sim}{s}) \rangle = f_1(z,u;\rho^2)\ \underset{\sim}{\rho}\ \underset{\sim}{\rho} + f_2(z,u;\rho^2)\ \underset{\sim}{\delta} \quad , \tag{26}$$

where $\underset{\sim}{\delta} = \underset{\sim}{e}_x\ \underset{\sim}{e}_x + \underset{\sim}{e}_y\ \underset{\sim}{e}_y$ with $\underset{\sim}{e}_x$ and $\underset{\sim}{e}_y$ being the unit vectors in the transverse plane. The function f_1 and f_2 are unspecified; they are used here to illustrate the functional dependence on variables z, u and ρ.

From equations (25) and (26), we deduce:

$$\underset{\sim}{\nabla}_r . \langle \underset{\sim}{v}(z,\underset{\sim}{r})\ \underset{\sim}{v}(u,\underset{\sim}{s}) \rangle = - \left\{ \rho\ \frac{\partial f_1}{\partial \rho} + \frac{1}{\rho}\ \frac{\partial f_2}{\partial \rho} + 3 f_1 \right\} \underset{\sim}{\rho} \quad . \tag{27}$$

Upon substituting this relation in equation (24) and using (19), we find for $\langle a\underset{\sim}{\nabla}.\underset{\sim}{v}\rangle$:

$$\langle a\underset{\sim}{\nabla}.\underset{\sim}{v}\rangle = \frac{ik}{2\pi}\int_0^z \frac{du}{(u-z)} \iint_{-\infty}^{\infty} d^2\underset{\sim}{\rho}\, \exp\left[\frac{ik}{2(z-u)}\,\frac{(F-z)}{(F-u)}\,\rho^2\right]\left\{\rho\,\frac{\partial f_1}{\partial\rho}+\frac{1}{\rho}\,\frac{\partial f_2}{\partial\rho}+3f_1\right\}\underset{\sim}{\rho}.\underset{\sim}{\nabla}_s\langle A\rangle$$

$$+\frac{ik}{4\pi}\int_0^z \frac{du}{(u-z)} \iint_{-\infty}^{\infty} d^2\underset{\sim}{\rho}\, \exp\left[\frac{ik}{2(z-u)}\,\frac{(F-z)}{(F-u)}\,\rho^2\right]\underset{\sim}{\nabla}_\rho\underset{\sim}{\nabla}_\rho:\langle\underset{\sim}{v}(z,\underset{\sim}{r})\;\underset{\sim}{v}(u,\underset{\sim}{s})\rangle\,\langle A(u,\underset{\sim}{s})\rangle. \tag{28}$$

Since the scales of the average amplitude are much greater than those of the correlation function of $\underset{\sim}{v}$ or, in the transverse plane, much greater than $\sqrt{2(z-u)\lambda}$, the quantities $\langle A(u,\underset{\sim}{s})\rangle$ and $\underset{\sim}{\nabla}_s\langle A(u,\underset{\sim}{s})\rangle$ can be taken out of the integral operators in equation (28). Then, the integrand of the first term on the right-hand side of equation (28) has the form of a function of ρ^2 multiplied by the vector $\underset{\sim}{\rho}$. Since integration is over the complete plane or over 2π radians, this first term vanishes and we are left with:

$$\langle a.\underset{\sim}{\nabla}\underset{\sim}{v}\rangle = K(z)\;\langle A\rangle \quad , \tag{29}$$

where:

$$K(z) = \frac{ik}{4\pi}\int_0^z \frac{du}{(u-z)} \iint_{-\infty}^{\infty} d^2\underset{\sim}{\rho}\, \exp\left[\frac{ik}{2(z-u)}\,\frac{(F-z)}{(F-u)}\,\rho^2\right]\underset{\sim}{\nabla}_\rho\underset{\sim}{\nabla}_\rho:\langle\underset{\sim}{v}(z,\underset{\sim}{r})\;\underset{\sim}{v}(u,\underset{\sim}{r}+\underset{\sim}{\rho})\rangle \quad . \tag{30}$$

The function $K(z)$ is independent of transverse position $\underset{\sim}{r}$ because of the hypothesis of statistical homogeneity of $\underset{\sim}{v}$ in the plane normal to the propagation axis.

An analogous procedure is used to derive the constitutive relation for $\langle \underset{\sim}{v} a \rangle$. Multiplying equation (19) by $\underset{\sim}{v}$ and taking the ensemble average, we obtain, under the integral signs, the following expression:

$$\begin{aligned}\langle \underset{\sim}{v}(z,\underset{\sim}{r})\, g(u,\underset{\sim}{s})\rangle = &-\langle \underset{\sim}{v}(z,\underset{\sim}{r})\, \underset{\sim}{v}(u,\underset{\sim}{s})\rangle .\, \underset{\sim}{\nabla}_{\underset{\sim}{s}} \langle A(u,\underset{\sim}{s})\rangle \\ &- \tfrac{1}{2}\langle A(u,\underset{\sim}{s})\rangle\, \underset{\sim}{\nabla}_{\underset{\sim}{s}} .\langle \underset{\sim}{v}(u,\underset{\sim}{s})\, \underset{\sim}{v}(z,\underset{\sim}{r})\rangle \\ &- \underset{\sim}{\nabla}_{\underset{\sim}{s}} .\langle \underset{\sim}{v}(u,\underset{\sim}{s})\, \underset{\sim}{v}(z,\underset{\sim}{r})\, a(u,\underset{\sim}{s})\rangle \\ &+ \tfrac{1}{2}\, \langle \underset{\sim}{v}(z,\underset{\sim}{r})\, a(u,\underset{\sim}{s})\, \underset{\sim}{\nabla}_{\underset{\sim}{s}} .\underset{\sim}{v}(u,\underset{\sim}{s})\rangle \quad . \end{aligned} \tag{31}$$

Neglecting the third-order moments in accordance with our second hypothesis and using equations (25) and (26), we find:

$$\begin{aligned}\langle \underset{\sim}{v}(z,\underset{\sim}{r})\, g(u,\underset{\sim}{s})\rangle = &- \langle v(z,\underset{\sim}{r})\, \underset{\sim}{v}(u,\underset{\sim}{s})\rangle .\underset{\sim}{\nabla}_{\underset{\sim}{s}} \langle A(u,\underset{\sim}{s})\rangle \\ &- \tfrac{1}{2}\left\{ \rho\, \frac{\partial f_1}{\partial \rho} + \frac{1}{\rho}\, \frac{\partial f_2}{\partial \rho} + 3 f_1 \right\} \underset{\sim}{\rho}\, \langle A(u,\underset{\sim}{s})\rangle \quad . \end{aligned} \tag{32}$$

Following the same steps as before, we obtain:

$$\langle \underset{\sim}{v} a\rangle = - R(z)\, \underset{\sim}{\nabla} \langle A\rangle \quad , \tag{33}$$

where:

$$R(z) = \frac{ik}{4\pi} \int_0^z \frac{du}{(u-z)} \iint_{-\infty}^{\infty} d^2\underset{\sim}{\rho}\, \exp\left[\frac{ik}{2(z-u)}\, \frac{(F-z)}{(F-u)}\, \rho^2 \right] \langle \underset{\sim}{v}(z,\underset{\sim}{r}) .\underset{\sim}{v}(u,\underset{\sim}{r}+\underset{\sim}{\rho})\rangle \quad . \tag{34}$$

Use was made of equation (26) to reduce the proportionality function R(z) to a scalar.

The same derivation technique is used for the remaining terms $\langle \underset{\sim}{v}aa \rangle$ and $\langle \underset{\sim}{v}aa^* \rangle$. After multiplication of equation (19) by $\underset{\sim}{v}a$, the expression under the integral operator becomes:

$$\begin{aligned}\langle \underset{\sim}{v}(z,\underset{\sim}{r})\, a(z,\underset{\sim}{r})\, a(u,\underset{\sim}{s}) \rangle = &- \langle \underset{\sim}{v}(z,\underset{\sim}{r})\, a(z,\underset{\sim}{r})\, \underset{\sim}{v}(u,\underset{\sim}{s}) \rangle \,.\underset{\sim}{\nabla}_s \langle A(u,\underset{\sim}{s}) \rangle \\ &- \tfrac{1}{2}\, \underset{\sim}{\nabla}_s . \langle \underset{\sim}{v}(u,\underset{\sim}{s})\, \underset{\sim}{v}(z,\underset{\sim}{r})\, a(z,\underset{\sim}{r}) \rangle \langle A(u,\underset{\sim}{s}) \rangle \\ &- \underset{\sim}{\nabla}_s . \langle \underset{\sim}{v}(u,\underset{\sim}{s})\, a(u,\underset{\sim}{s})\, \underset{\sim}{v}(z,\underset{\sim}{r})\, a(z,\underset{\sim}{r}) \rangle \\ &+ \tfrac{1}{2} \langle \underset{\sim}{v}(z,\underset{\sim}{r})\, a(z,\underset{\sim}{r})\, a(u,\underset{\sim}{s})\, \underset{\sim}{\nabla}_s . \underset{\sim}{v}(u,\underset{\sim}{s}) \rangle \quad . \end{aligned} \tag{35}$$

From equations (20 b and c) we obtain to the order of $\langle \underset{\sim}{v}.\underset{\sim}{v} \rangle$ and, after rearranging:

$$\begin{aligned}\langle \underset{\sim}{v}(z,\underset{\sim}{r})\, a(z,\underset{\sim}{r})\, a(u,\underset{\sim}{s}) \rangle = &- \langle \underset{\sim}{v}(z,\underset{\sim}{r})\, \underset{\sim}{v}(u,\underset{\sim}{s}) \rangle . \underset{\sim}{\nabla}_s \langle a(u,\underset{\sim}{s})\, a(z,\underset{\sim}{r}) \rangle \\ &- \tfrac{1}{2} \langle a(u,\underset{\sim}{s})\, a(z,\underset{\sim}{r}) \rangle \underset{\sim}{\nabla}_s . \langle \underset{\sim}{v}(u,\underset{\sim}{s})\, \underset{\sim}{v}(z,\underset{\sim}{r}) \rangle \quad . \end{aligned} \tag{36}$$

Using equations (21), (25), (26) and (36) and following the same steps as before, we find:

$$\langle \underset{\sim}{v}aa \rangle = - \tfrac{1}{2}\, P(z)\, \underset{\sim}{\nabla} \langle aa \rangle \quad , \tag{37}$$

where:

$$P(z) = \frac{ik}{4\pi}\int_0^z \frac{du}{(u-z)} \iint_{-\infty}^{\infty} d^2\underset{\sim}{\rho} \quad \exp\left[\frac{ik}{2(z-u)}\frac{(F-z)}{(F-u)}\rho^2\right] <\underset{\sim}{v}(z,\underset{\sim}{r}).\underset{\sim}{v}(u,\underset{\sim}{r}+\underset{\sim}{\rho})>g_{aa}(z,u;\rho) \tag{38}$$

Similarly, starting with $\frac{1}{2}[<\underset{\sim}{v}(z,\underset{\sim}{r})\ a^*(z,\underset{\sim}{r})\ g(u,\underset{\sim}{s})> + <\underset{\sim}{v}(z,\underset{\sim}{r})\ a(z,\underset{\sim}{r})g^*(u,\underset{\sim}{s})>]$, we obtain:

$$<\underset{\sim}{v}aa^*> = -\ \tfrac{1}{2}\ Q(z)\ \underset{\sim}{\nabla}\ <aa^*> \quad , \tag{39}$$

where:

$$Q(z) = \text{Real}\left\{\frac{ik}{4\pi}\int_0^z \frac{du}{(u-z)} \iint_{-\infty}^{\infty} d^2\underset{\sim}{\rho} \quad \exp\left[\frac{ik}{2(z-u)}\frac{(F-z)}{(F-u)}\rho^2\right] <\underset{\sim}{v}(z,\underset{\sim}{r}).\underset{\sim}{v}(u,\underset{\sim}{r}+\underset{\sim}{\rho})> \times g_{aa^*}(z,u;\rho)\right\} \quad . \tag{40}$$

3.3 Discussion

We have derived equations that relate in closed form the higher order unknown moments of equations (9) to (11) to the lower order amplitude moments for which a solution is sought. These relations constitute the principal result of this report and, for easy reference, they are regrouped together below:

$$<a\underset{\sim}{\nabla}.\underset{\sim}{v}> = -\ K(z)\ \ <A> \quad , \tag{29}$$

$$\langle \underset{\sim}{v}a \rangle = - R(z)\, \underset{\sim}{\nabla} \langle A \rangle \quad , \tag{33}$$

$$\langle \underset{\sim}{v}aa \rangle = - \tfrac{1}{2} P(z)\, \underset{\sim}{\nabla} \langle aa \rangle \quad , \tag{37}$$

$$\langle \underset{\sim}{v}aa^* \rangle = -\tfrac{1}{2} Q(z)\, \underset{\sim}{\nabla} \langle aa^* \rangle \quad . \tag{39}$$

The proportionality functions are given by equations (30), (34), (38) and (40).

The approximations defined by the inequalities (20 a to c) form the basis of our model. If these were not satisfied, relations (29), (33), (37) and (39) would depend on cross-correlation moments of $\underset{\sim}{v}$ and a, and closure of the system of equations (9) to (11) would not be achieved. The validity of this weak correlation hypothesis will eventually have to be confirmed by direct measurements. However, equations (30), (34), (38) and (40) show that the hypothesis is self-consistent. Indeed, the proportionality functions vary as the volume integral of the covariance of $\underset{\sim}{v}$ which, for reasonable correlation lengths, should give results much smaller than the standard deviation of $\underset{\sim}{v}$.

A second hypothesis concerns isotropy of angle-of-arrival and quasi-isotropy of amplitude fluctuations in the transverse plane. The requirements here are that the surface integrals of the odd-order derivatives of scalar or second-order tensor covariance functions be much smaller than those of the even-order derivatives. This is a less stringent condition that does not require point by point verification. Moreover, since the major contributions to the integrals come from the neighbourhood of

$\underset{\sim}{\rho} = 0$, the hypothesis of isotropy can be relaxed to one of local isotropy, i.e. one that applies at a small separation distance only. Although convenient, the approximation could be abandoned without fundamental difficulties. This would simply mean the addition of one term in each of the constitutive relations: one term proportional to $\underset{\sim}{\nabla}\langle A\rangle$ in (29) and one term proportional to $\langle A\rangle$, $\langle aa\rangle$ and $\langle aa^*\rangle$ in (33), (37) and (39) respectively.

The functional relationships between the higher order and lower order moments in equations (29), (33), (37) and (39) are consistent with the physical interpretation of the terms they model. The beam breakup term, $\langle a\underset{\sim}{\nabla}.\underset{\sim}{v}\rangle$, is proportional to the average amplitude and, therefore, it survives for plane waves, as indeed it should. The terms responsible for beam spreading, i.e. $\langle \underset{\sim}{v}a\rangle$, $\langle \underset{\sim}{v}aa\rangle$ and $\langle \underset{\sim}{v}aa^*\rangle$, are all proportional to gradients of the corresponding lower order mean field quantity and, as expected, they vanish for plane waves. The latter relations are analogous with expressions successfully used to model the turbulent momentum, heat and mass transport terms in turbulent shear flows e.g. (Ref. 23).

To determine the functions K(z), R(z), P(z) and Q(z), we need expressions for the covariance function $\langle \underset{\sim}{v}(z,\underset{\sim}{r})\ \underset{\sim}{v}(u,\underset{\sim}{r}+\underset{\sim}{\rho})\rangle$ and for the correlation functions $g_{aa}(z,u;\rho)$ and $g_{aa^*}(z,u;\rho)$. By assumption of statistical homogeneity for $\underset{\sim}{v}$ and of quasi-homogeneity for a, the functions $\langle \underset{\sim}{v}\underset{\sim}{v}\rangle$, g_{aa} and g_{aa^*} are independent of beam geometry. Hence, it is necessary to solve them for plane waves only and, after substitution in equations

(30), (34), (38) and (40), the resulting functions K(z), R(z), P(z) and Q(z) are applicable to any beam geometry. Therefore, the present approach conveniently dissociates or separates the turbulence problem from that of geometry as is the case with the Extended Huygens-Fresnel method of Ref. 12.

Solutions for the phase and amplitude correlation functions of a plane wave are already known. However, they are all specialized to displacements in the transverse plane only. This is not sufficient for the present purpose and new developments regarding longitudinal dependence are required. Instead of trying to solve this problem exactly here, we will proceed indirectly and use simple known theoretical results along with some empirical data. Comparison with measurements will show that this simpler approach is very satisfactory for practical applications.

4.0 SEMI-EMPIRICAL MODEL

4.1 Proportionality Functions

The approach we will follow to determine the proportionality function is indirect or empirical. It is based on the requirement that our solution for the irradiance variance σ_I^2 should match the theoretical weak perturbation solution in the limit of small propagation distance. Since the plane wave solution of equations (9) to (11) depends on function K(z) only, it is convenient to start with this simpler situation.

Substituting equation (29) for the beam breakup term in equations (9) to (11) and making the hypothesis of normal probability distribution for the complex wave amplitude, which will be discussed later in this report, we obtain the following plane wave solution valid in the limit of small z:

$$\sigma_I^2 = 4 \int_o^z K(z)\, dz \quad . \tag{41}$$

The corresponding perturbation result is the Rytov formula for plane waves given by (Ref. 2):

$$\sigma_R^2 = 1.24 \frac{C_n^2}{n_o^2} k^{7/6} z^{11/6} \quad . \tag{42}$$

Equating (41) to (42) and taking the z-derivative, we find:

$$K(z) = 0.568 \frac{C_n^2}{n_o^2} k^{7/6} z^{5/6} \quad . \tag{43}$$

Strictly speaking, equation (43) is valid in the weak-scintillation region. However, since K(z) depends on phase-related functions only, as shown by equation (30), and since perturbation results regarding phase statistics are known to apply well into the strong-scintillation region (Refs. 24-26), we simply extend the validity of equation (43) to large values of propagation distance without modification. Results will show a posteriori that the approximation is justified.

For propagation distances $z<<\ell_o^2/\lambda$, where ℓ_o is the inner scale of turbulence and λ the radiation wavelength, the Rytov formula must be replaced by the geometrical optics formula (Ref. 2), i.e.:

$$\sigma^2_{g\text{-}o} = 12.8 \frac{C_n^2 z^3}{n_o^2 \ell_o^{7/3}} \quad ; \quad z<<\ell_o^2/\lambda \quad , \tag{44}$$

from where we derive:

$$K(z) = 9.60 \frac{C_n^2 z^2}{n_o^2 \ell_o^{7/3}} \quad ; \quad z<<\ell_o^2/\lambda \quad . \tag{45}$$

The connecting region between geometrical and diffractional optics is not modelled by a simple algebraic relation. For the present purpose, we assume an abrupt passage between regions of validity of equations (43) and (45) and obtain the point of separation as the distance $z=z_o$ at which expressions (43) and (45) become equal. We thus find:

$$z_o = 0.557 \ \ell_o^2/\lambda \quad , \tag{46}$$

and the function K(z) is defined as follows:

$$K(z) = \begin{cases} 9.60 \dfrac{C_n^2 z^2}{n_o^2 \ell_o^{7/3}} \quad ; \quad z \leq z_o \quad , & \text{(47a)} \\ 0.568 \dfrac{C_n^2}{n_o^2} k^{7/6} z^{5/6} \quad ; \quad z > z_o \quad . & \text{(47b)} \end{cases}$$

This matching is very unsophisticated but adequate as the results will show.

There is no simple small perturbation solution for finite beams from which R(z) could be determined in the same manner as with K(z). The procedure adopted is to derive an approximate algebraic relation between R(z) and the already known K(z) from examination of their respective functional dependence given by equations (30) and (34). These equations are of the same form, i.e. the same integral operator applied to the covariance functions $\nabla_{\rho}\nabla_{\rho}:\langle \underset{\sim}{v}(z,\underset{\sim}{r})\ \underset{\sim}{v}(u,\underset{\sim}{r}+\underset{\sim}{\rho})\rangle$ and $\langle \underset{\sim}{v}(z,\underset{\sim}{r}).\underset{\sim}{v}(u,\underset{\sim}{r}+\underset{\sim}{\rho})\rangle$ respectively. Approximations for the latter can be derived from the theoretical expression for the phase structure function (Ref. 1):

$$D_{\phi}(\rho) = 3.44\ \frac{C_n^2\ \rho^2}{n_o^2 \ell_o^{1/3}}\ z \quad ; \quad \rho < \ell_o \quad . \tag{48a}$$

$$D_{\phi}(\rho) = 2.91\ \frac{C_n^2\ \rho^{5/3}}{n_o^2}\ z \quad ; \quad \rho > \ell_o \quad . \tag{48b}$$

From the definition of vector $\underset{\sim}{V}$, there follows:

$$\langle \underset{\sim}{v}.\underset{\sim}{v}\rangle \simeq 3.44\ \frac{C_n^2\ z}{n_o^2 \ell_o^{1/3}} \quad , \tag{49}$$

$$\lim_{\rho\to 0}\ \nabla_{\rho}\nabla_{\rho}:\ \langle \underset{\sim}{v}(z,\underset{\sim}{r})\ \underset{\sim}{v}(z,\underset{\sim}{r}+\underset{\sim}{\rho})\rangle \simeq 0.72\ \frac{C_n^2\ z}{n_o^2 \ell_o^{7/3}} \quad , \tag{50}$$

$$\frac{\langle \underset{\sim}{v}(z,\underset{\sim}{r}) \cdot \underset{\sim}{v}(z,\underset{\sim}{r}+\underset{\sim}{\rho}) \rangle}{\langle \underset{\sim}{v} \cdot \underset{\sim}{v} \rangle} \sim (\rho/\ell_o)^{-1/3} \qquad \rho > \ell_o \quad , \tag{51}$$

$$\frac{\underset{\sim}{\nabla}_\rho \underset{\sim}{\nabla}_\rho : \langle \underset{\sim}{v}(z,\underset{\sim}{r})\ \underset{\sim}{v}(z,\underset{\sim}{r}+\underset{\sim}{\rho}) \rangle}{\lim_{\rho \to 0} \underset{\sim}{\nabla}_\rho \underset{\sim}{\nabla}_\rho : \langle \underset{\sim}{v}(z,\underset{\sim}{r})\ \underset{\sim}{v}(z,\underset{\sim}{r}+\underset{\sim}{\rho}) \rangle} \sim (\rho/\ell_o)^{-7/3} \quad ; \quad \rho > \ell_o \quad . \tag{52}$$

Of particular interest here is the large difference between the decay rates of the correlation functions given by equations (51) and (52). These rates are to be compared with the period of oscillation of the complex exponential in the integral operator of equations (30) and (34). In the first case, i.e. equation (30), the exponential undergoes only a few oscillations, except near u=z, before the correlation function becomes negligibly small. Exactly the opposite occurs in the second case, i.e. equation (34); the exponential oscillates very rapidly compared with the decay rate of the correlation function. Assuming that the power laws given by equations (51) and (52) are representative of the true transverse variation of the correlation functions at nonzero longitudinal separation, we conclude that the surface integral of equation (34) scales roughly as the square of the period of oscillation of the complex exponential and that of equation (30) as ℓ_o^2. Therefore, we approximate R(z) as follows:

$$R(z) \simeq K(z)\ \frac{2\ell}{k\ell_o^2} \left\{ \frac{\langle \underset{\sim}{v}(z,\underset{\sim}{r}) \cdot \underset{\sim}{v}(z,\underset{\sim}{r}) \rangle}{\lim_{\rho \to 0} \underset{\sim}{\nabla}_\rho \underset{\sim}{\nabla}_\rho : \langle \underset{\sim}{v}(z,\underset{\sim}{r})\ \underset{\sim}{v}(z,\underset{\sim}{r}+\underset{\sim}{\rho}) \rangle} \right\} \quad , \tag{53}$$

where ℓ is the longitudinal correlation length of $\langle \underset{\sim}{v}(z,\underset{\sim}{r}).\underset{\sim}{v}(u,\underset{\sim}{r}+\underset{\sim}{\rho})\rangle$. There are no theoretical nor experimental data on ℓ so all we can do here is to rely on a posteriori confirmation. We simply assume that ℓ is proportional to propagation distance and from equations (49), (50), and (53), we obtain:

$$R(z) = \gamma \frac{z}{k} K(z) \quad , \tag{54}$$

where γ is an empirical constant to be determined by measurements.

The functions P(z) and Q(z) differ from R(z) by the presence of the correlation functions g_{aa} and g_{aa^*} under the integral signs of equations (38) and (40). On an order-of-magnitude basis, we assume that the transverse scales, for small separation distances, of the correlation functions g_{aa} and g_{aa^*} are equal and can be approximated by the amplitude-correlation length for zero longitudinal separation. The latter initially increases as $\sqrt{\lambda z}$, passes through a maximum near $z = z_A = n_o^{12/11} / C_n^{12/11} k^{7/11}$ and then decreases proportionally to the coherence radius $\rho_o = [1.45\ C_n^2\ k^2 z]^{-3/5}$ of the Mutual Coherence Function (Ref. 13); z_A is the propagation scale at which the coherent amplitude $\langle A \rangle$ has decreased by a factor 1/e. For $z<z_A$, this means that the surface integrals in equations (38) and (40) depend only weakly on the lateral variation of g_{aa} and g_{aa^*} since the period of oscillation of the complex exponential appearing in equations (38) and (40), i.e. $\sqrt{2(z-u)\lambda}$, is much smaller than $\sqrt{\lambda z}$. For $z>z_A$, Figs. 3-5 of Ref. 13 show that the amplitude-correlation

length, although decreasing with increasing z, remains of the order of $\sqrt{\lambda z}$ well into the strong scintillation region. Hence, we assume that P(z) and Q(z) remain practically independent of the lateral variation of g_{aa} and g_{aa^*} for all propagation distances of interest and, therefore, we can use equation (53) to relate P(z) and Q(z) to K(z). The longitudinal scale ℓ is not necessarily the same for P(z), Q(z) and R(z) but, in the absence of better information and to minimize the number of adjustable empirical constants, we simply make:

$$P(z) \simeq Q(z) \simeq R(z) \quad . \tag{55}$$

The simple algebraic equations (47), (54) and (55) constitute an empirical determination of the proportionality functions K(z), R(z), P(z) and Q(z). They are based on heuristic arguments and the final justification must come from comparison with measurements. Strictly speaking, equations (47) and (54) apply to collimated beams only. They will have to be revised for focused beams, especially near the focal region. This will be done as soon as we have sufficient and varied data to compare them with.

There remains to model the moment $\langle \underset{\sim}{\nabla} a . \underset{\sim}{\nabla} a \rangle$. From the hypothesis of quasi-homogeneity and quasi-isotropy, we have:

$$\langle \underset{\sim}{\nabla} a . \underset{\sim}{\nabla} a \rangle = - \langle aa \rangle \lim_{\rho \to 0} \frac{\partial^2}{\partial \rho^2} g_{aa}(z,z;\rho) \quad , \tag{56}$$

For $z>z_A$, Yura (Ref. 13) has shown that the characteristic amplitude coherence scale is proportional to the coherence radius ρ_o. Assuming that, for ρ not too large, g_{aa} has the same functional dependence as the Mutual Coherence Function, i.e. $\exp[-(\rho/\rho_o)^{5/3}]$, and matching at $\rho=\rho_m$ this function to the quadratic expansion valid near $\rho=0$, we have:

$$\lim_{\rho\to 0} \frac{\partial^2}{\partial\rho^2} g_{aa} = -C' \rho_m^{-1/3} \rho_o^{-5/3} \quad , \tag{57}$$

where C' is an empirical constant. The matching radius ρ_m is unknown but, given the weak dependence of equation (57) on ρ_m, we should make only a negligible error by assuming that it is constant with respect to propagation distance. However, ρ_m should depend on turbulence condition and wavelength; the simplest expression that satisfies these conditions is $\rho_m^2 \sim \lambda z_A$. Using equation (57) with $\rho_o = [1.45\, C_n^2\, k^2 z/n_o^2]^{-3/5}$ and $z_A = n_o^{12/11}/C_n^{12/11}\, k^{7/11}$, and regrouping the constants, we thus obtain:

$$\langle \nabla a . \nabla a \rangle = C \frac{kz}{z_A^2} \langle aa \rangle \quad . \tag{58}$$

Equation (58) is applicable for $z>z_A$ only. However, calculations have shown that $\langle \nabla a . \nabla a \rangle$ has little bearing on numerical results in the weak-scintillation region. For this reason, equation (58) is used for all values of z without modification. C is a second empirical constant and, since g_{aa} is complex, C is also complex although its imaginary part is expected to be much smaller than its real part.

Finally, from equations (21b) and (22b), we find:

$$\langle a^* \underset{\sim}{\nabla} a \rangle - \langle a \underset{\sim}{\nabla} a^* \rangle = 0 \quad . \tag{59}$$

4.2 Model Equations

The propagation distance is normalized by z_A, i.e. $\eta = z/z_A$, and the transverse coordinates by r_o. After substitution of equations (29), (33), (37), (39), (58) and (59) for the unknown moments, we obtain a closed set of simultaneous linear partial differential equations of second order for $\langle A \rangle$, $\langle aa \rangle$ and $\langle aa^* \rangle$. They are written here for collimated beams:

$$\frac{\partial}{\partial \eta} \langle A \rangle + \tfrac{1}{2} K(\eta) \langle A \rangle - b[R(\eta) + \frac{i}{2}] \underset{\sim}{\nabla}^2 \langle A \rangle = 0 \quad , \tag{60}$$

$$\frac{\partial}{\partial \eta} \langle aa \rangle + i\, T(\eta) \langle aa \rangle - \frac{b}{2} [R(\eta) + i] \underset{\sim}{\nabla}^2 \langle aa \rangle$$

$$= 2\, bR(\eta) \underset{\sim}{\nabla} \langle A \rangle . \underset{\sim}{\nabla} \langle A \rangle + K(\eta) \langle A \rangle^2 \quad , \tag{61}$$

$$\frac{\partial}{\partial \eta} \langle aa^* \rangle - \tfrac{1}{2}\, b\, R(\eta)\, \underset{\sim}{\nabla}^2 \langle aa^* \rangle$$

$$= 2\, b\, R(\eta) \underset{\sim}{\nabla} \langle A \rangle . \underset{\sim}{\nabla} \langle A \rangle^* + K(\eta) \langle A \rangle \langle A \rangle^* \quad . \tag{62}$$

The gradient operator is with respect to the normalized coordinate $\underset{\sim}{r}/r_o$.

The non-dimensional functions $K(\eta)$, $R(\eta)$ and $T(\eta)$ are given by

the following simple algebraic functions of the normalized propagation distance:

$$K(\eta) = \begin{cases} 0.568\ \eta^2/\eta_o^{7/6} \ ; & \eta \leq \eta_o \quad , \qquad (63a) \\ 0.568\ \eta^{5/6} \ ; & \eta > \eta_o \quad , \qquad (63b) \end{cases}$$

$$R(\eta) = \gamma\eta\ K(\eta) \quad , \qquad (64)$$

$$T(\eta) = C\eta \quad . \qquad (65)$$

There are two similarity parameters:

$$\eta_o = \frac{0.557}{2\pi} \quad \frac{k\ell_o^2}{z_A} \quad , \qquad (66)$$

$$b = \frac{z_A}{kr_o^2} \quad . \qquad (67)$$

The parameter η_o appears only in $K(\eta)$ and for $\eta<\eta_o$. If η_o is small, as in many atmospheric applications, we can neglect (63a) and use (63b) for the complete propagation range. In this case, solutions are independent of η_o or, in dimensional form, they are independent of the inner scale ℓ_o.

A very important practical quantity that needs to be treated is the irradiance variance defined as follows:

$$\sigma_I^2 = \langle aa^*aa^* \rangle + 2\langle A \rangle \langle aa^*a^* \rangle$$

$$+ 2\langle A \rangle^* \langle a^*aa \rangle - \langle aa^* \rangle^2 + 2\langle A \rangle \langle A \rangle^* \langle aa^* \rangle$$

$$+ \langle A \rangle \langle A \rangle \langle aa \rangle^* + \langle A \rangle^* \langle A \rangle^* \langle aa \rangle \quad . \tag{68}$$

Equation (68) shows that σ_I^2 depends on amplitude moments of order three and four which are not included in the present model. To write σ_I^2 in terms of $\langle A \rangle$, $\langle aa \rangle$ and $\langle aa^* \rangle$, we make the hypothesis of normal probability distribution of the random complex amplitude, a. This approximation is based on the application of the central limit theorem to the solution for the fluctuating amplitude obtained from equations (18) and (19) and shown here for collimated beams:

$$a(z,\underset{\sim}{r}) = \frac{ik}{2\pi} \int_0^z \frac{du}{(u-z)} \iint_{-\infty}^{\infty} d^2\underset{\sim}{s} \exp\left[\frac{ik}{2(z-u)} \left|\underset{\sim}{s}-\underset{\sim}{r}\right|^2\right]$$

$$\times \left\{-\underset{\sim}{v}.\underset{\sim}{\nabla}\langle A \rangle - \tfrac{1}{2} \langle A \rangle \underset{\sim}{\nabla}.\underset{\sim}{v} - \tfrac{1}{2}[a\underset{\sim}{\nabla}.\underset{\sim}{v} - \langle a\underset{\sim}{\nabla}.\underset{\sim}{v} \rangle] - [\underset{\sim}{v}.\underset{\sim}{\nabla}a - \langle \underset{\sim}{v}.\underset{\sim}{\nabla}a \rangle]\right\} \tag{69}$$

In the weak-scintillation regime, the linear random terms $\underset{\sim}{v}.\underset{\sim}{\nabla}\langle A \rangle$ and $\frac{1}{2}\langle A \rangle \underset{\sim}{\nabla}.\underset{\sim}{v}$ dominate. Neglecting diffraction (i.e. $k \to \infty$), we have at small values of z:

$$a(z,\underset{\sim}{r}) \simeq \int_0^z du \left\{-\underset{\sim}{v}.\underset{\sim}{\nabla}\langle A \rangle - \tfrac{1}{2}\langle A \rangle \underset{\sim}{\nabla}.\underset{\sim}{v}\right\} \quad . \tag{70}$$

Hence, providing that the longitudinal correlation length of $\underset{\sim}{v}$ is small

compared with propagation distance, the fluctuating amplitude results from the sum of many independent random processes and the central limit theorem suggests that $a(z,\underset{\sim}{r})$ is normally distributed. As propagation distance or turbulence strength increases, the nonlinear random terms become dominant. The first of these terms, $\frac{1}{2}a\underset{\sim}{\nabla}.\underset{\sim}{v}$, gives in the geometrical optics limit:

$$\ell n\ a(z,\underset{\sim}{r}) \sim -\frac{1}{2}\int_0^z du\ \underset{\sim}{\nabla}.\underset{\sim}{v} \quad . \tag{71}$$

Thus, the contribution from $\frac{1}{2}a\underset{\sim}{\nabla}.\underset{\sim}{v}$ indicates a log-normal distribution. However, the effect of the accompanying nonlinear term, $\underset{\sim}{v}.\underset{\sim}{\nabla}a$, is additive. Indeed, this term represents turbulence scattering from many different regions off the line-of-sight; it is the multiple-path effect described by Strohbehn et al. (Ref. 27). Hence, this second nonlinear term suggests a normal distribution for the complex amplitude and, as far as we can tell, it is of the same order of magnitude as $\frac{1}{2}a\underset{\sim}{\nabla}.\underset{\sim}{v}$. Finally, equation (69) shows that, for $2\lambda(z-u)>\ell_o^2$, the mechanisms leading to fluctuations of the complex amplitude and described above are all subject to diffraction scattering from the turbulent regions off the optical axis. The latter effect is additive and further supports Gaussian statistics for the complex amplitude. Therefore, the turbulence mechanisms of equation (69) favour in majority a normal over a log-normal probability distribution for the complex wave amplitude A defined by equation (1).

The assumption of Gaussian statistics for the complex wave amplitude gives:

$$\langle aa^*a^* \rangle = \langle a^*aa \rangle = 0 \quad , \tag{72}$$

$$\langle aa^*aa^* \rangle = 2\langle aa^* \rangle^2 + \langle aa \rangle \langle aa \rangle^* \quad , \tag{73}$$

from where we obtain:

$$\sigma_I^2 = \langle aa^* \rangle^2 + \langle aa \rangle \langle aa \rangle^* + 2\langle A \rangle \langle A \rangle^* \langle aa^* \rangle$$

$$+ \langle A \rangle \langle A \rangle \langle aa \rangle^* + \langle A \rangle^* \langle A \rangle^* \langle aa \rangle \quad . \tag{74}$$

The implications of the assumption of normal probability distribution for the complex wave amplitude are explicitly and completely specified by equations (72) and (73). Whether the amplitude moments of order higher than four can or cannot be separated according to Gaussian statistics is of no consequence here. Most importantly, the solutions to equations (60) to (62) are independent of this or any other probability hypothesis. Only the inference of the irradiance variance from these solutions, as given by equation (74), is dependent on the normal probability approximation.

5.0 EXPERIMENTAL VERIFICATION

5.1 Method of Solution

Equation (60) for the average amplitude is linear and uncoupled. An analytic solution is easily obtained in the case of an originally Gaussian beam. It is given by:

$$\langle A \rangle = f(\eta) \exp\left[-r^2/2r_o^2 h(\eta)\right] \quad , \tag{75}$$

where:

$$h(\eta) = 1 + ib\eta + 2b\int_o^\eta R(\eta)\, d\eta \quad , \tag{76}$$

$$f(\eta) = \frac{1}{h(\eta)} \exp\left[-\tfrac{1}{2}\int_o^\eta K(\eta)\, d\eta\right] \quad . \tag{77}$$

$R(\eta)$ and $K(\eta)$ being algebraic functions, the integrals in equations (76) and (77) are straightforward.

Equations (61) and (62) for $\langle aa \rangle$ and $\langle aa^* \rangle$ are linear but coupled with the average amplitude through their right-hand side terms. Closed-form solutions similar to equation (75) do not seem to exist. However, general solutions can be worked out in terms of Green's functions. These solutions involve multiple integrals. For Gaussian beams, the radial integration can be performed analytically but, even in this favourable

case, we are left with complicated longitudinal integrals that need to be evaluated numerically at each spatial point, since the radial dependence cannot be factored out. For this reason, we find it more convenient to solve the finite difference version of equations (60) to (62), which is fast and independent of beam geometry.

5.2 Determination of the Empirical Constants

To verify our model, a laboratory experiment was designed which allows complete control over the turbulence parameters. The experiment is fully described in Refs. 28 and 29 and is illustrated in Fig. 1. In short, the refractive index turbulences are produced by creating an unstable vertical temperature gradient in a tank filled with water. This is done simply by heating the water at the bottom of the tank and cooling it at the top. The tank is 1.5 m long, 0.6 m deep and 0.4 m wide. The propagation path is increased by folding the beam lengthwise as shown in Fig. 1. The Kolmogorov inertial subrange model is well verified and, typically, the index structure constant C_n is 10^{-4} $m^{-1/3}$.

Calculations have shown that the plane wave approximation, b=0, is valid for the on-axis normalized irradiance standard deviation, $\beta = \sigma_I/\langle I \rangle$, providing b is small enough, typically smaller than 0.01. We use this to determine C independently of γ since setting b=0 in equations (60) to (62) eliminates γ.

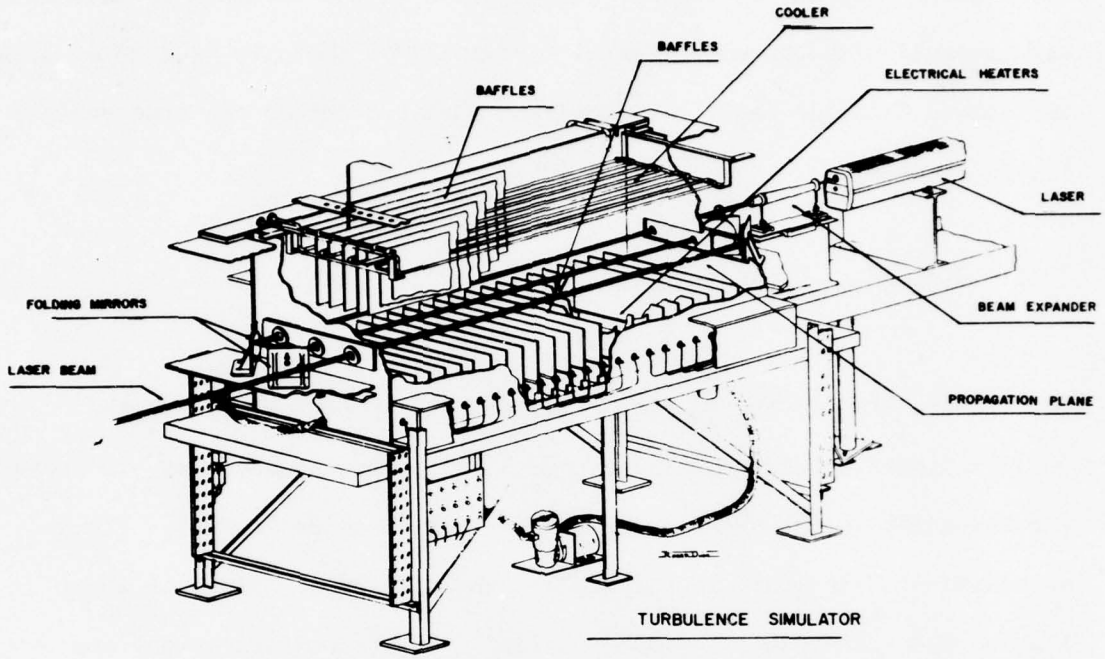

FIGURE 1 - Perspective drawing of the turbulence simulator

Equations (60) to (62) with b=0 were solved for various values of the complex constant C. The predicted plane wave β obtained in this manner was compared with the experimental β measured on the axis of a 25 mm diam collimated Gaussian beam. The constant C that produced the best overall fit is given by:

$$C = 0.31 - 0.01\ i \quad . \tag{78}$$

The results are plotted in Fig. 2 against the Rytov formula for the log-irradiance standard deviation, σ_R. Two theoretical curves are shown corresponding to the extreme values of η_o as given in Table I. The agreement is excellent; in particular, the predicted maximum of about 1.3 and the subsequent slow decay toward unity (supersaturation) are very well corroborated.

The constant γ is determined by a best fit to the on-axis average irradiance data. The results are shown in Fig. 3 where the solid curve represents the theoretical solution using:

$$\gamma = 2.8 \quad . \tag{79}$$

Without turbulence, the on-axis average irradiance would remain essentially equal to one for all propagation distances at which the measurements shown in Fig. 3 were taken. Hence, the turbulence-induced beam spread is important and it is accurately predicted by our model.

TABLE I

Experimental Conditions for Figs. 2-9

Fig. #	Symbol	k m^{-1}	r_o mm	ℓ_o mm	C_n $m^{-2/3}$	η_o	b
2	o	1.32×10^7	7.0	1.5	0.73×10^{-4}	2.0	.0020
2	Δ	1.32×10^7	7.0	1.5	0.96×10^{-4}	2.7	.0015
2	∇	1.32×10^7	7.0	1.5	1.24×10^{-4}	3.6	.0011
3	o	1.32×10^7	7.0	1.5	1.2×10^{-4}	3.5	.0012
4	o	1.32×10^7	3.0	1.5	1.2×10^{-4}	3.5	.0064
5-8	o	1.32×10^7	7.0	1.5	1.2×10^{-4}	3.5	.0012
9	o	1.00×10^7	150.	O(1.0)	$.8\text{-}8.0 \times 10^{-7}$	.0005-.006	.0007-.009

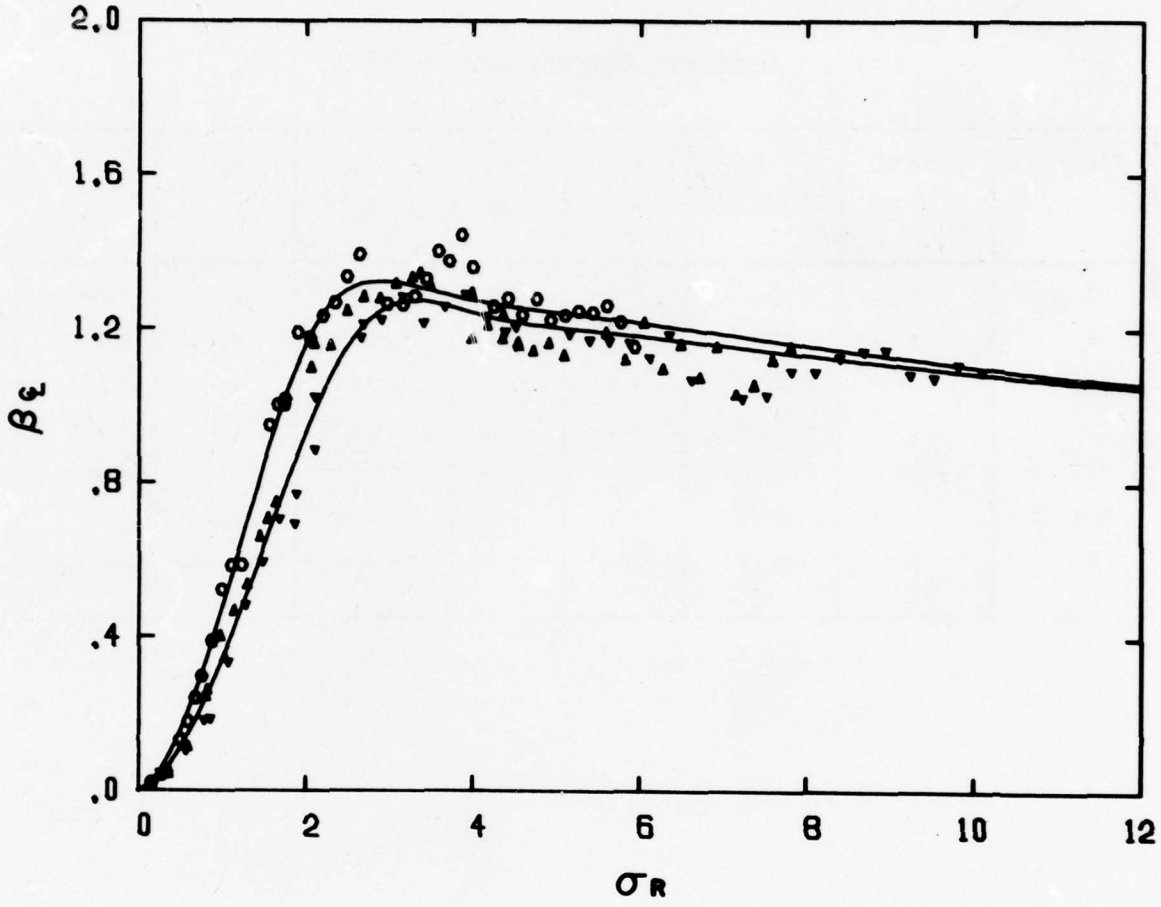

FIGURE 2 - The normalized irradiance standard deviation, $\beta=\sigma_I/\langle I\rangle$, measured on the axis of a 25 mm diam collimated laser beam plotted versus the Rytov formula for the log-irradiance standard deviation, σ_R. The experimental parameters for the corresponding symbols are listed in Table I. The solid curves are theoretical solutions for $\eta_o=2$ (upper curve) and $\eta_o=3.6$ (lower curve) obtained with the method of this paper.

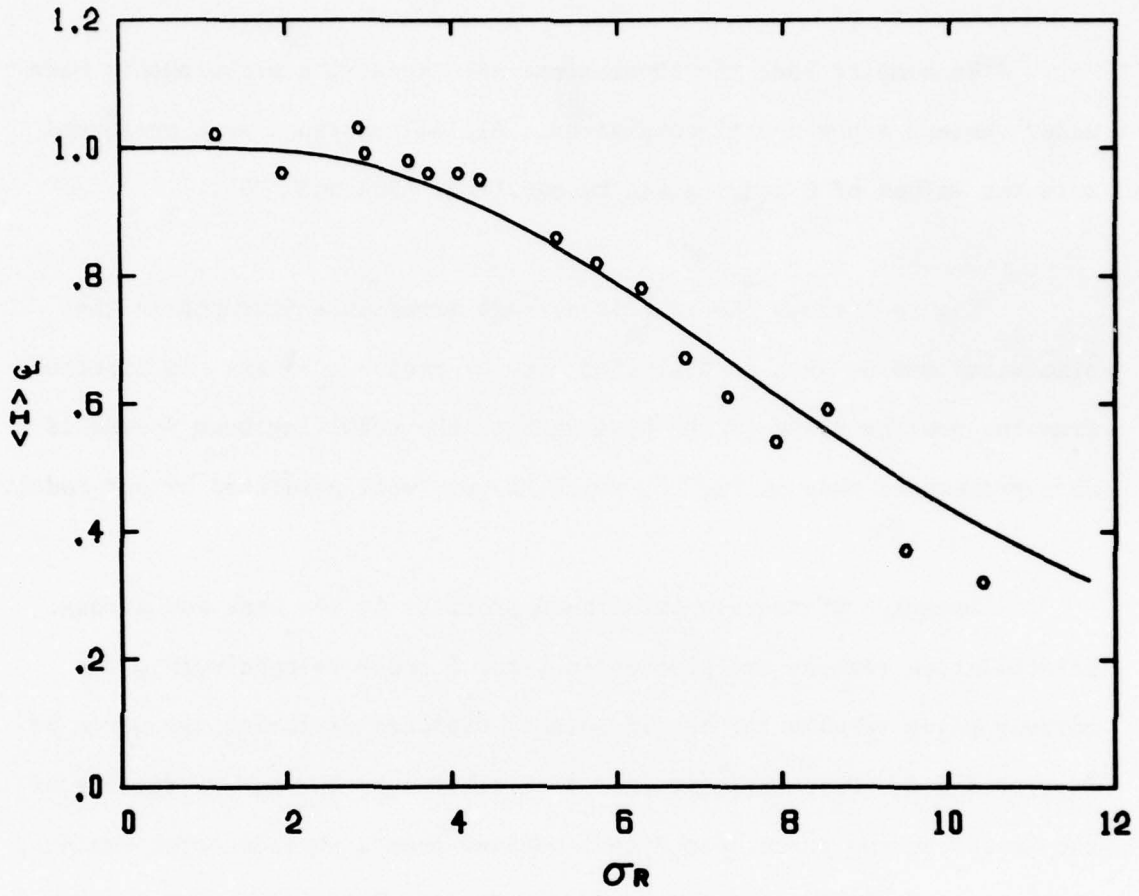

FIGURE 3 - The average irradiance measured on the axis of a 25 mm diam collimated laser beam plotted versus the Rytov formula for the log-irradiance standard deviation, σ_R. The experimental parameters are listed in Table I. The solid curve is the theoretical solution obtained with the method of this paper.

5.3 Universality of the Empirical Constants

We compare here the theoretical solutions with measurements made under various experimental conditions. All calculations were performed with the values of C and γ given by equations (78) and (79).

Figure 4 shows the on-axis average irradiance measured in the simulation medium with a collimated beam of radius r_o=3 mm. As expected from the smaller value of the beam radius, the resulting beam spread is more pronounced than in Fig. 3, which is very well predicted by our model.

Examples of average irradiance profiles in the weak and strong scintillation regions are plotted in Figs. 5 and 6 respectively. The corresponding results for the irradiance standard deviation are given in Figs. 7 and 8. Data were obtained from continuous DC and RMS records of the instantaneous irradiance signal derived from a photodetector scanning the beam very slowly, about 0.02 mm/s. In all cases, agreement between theory and measurements is very good. Experimental errors are approximately 10 to 15% of on-axis values. These relatively large errors are due to the very sharp irradiance peaks that are characteristic of optical scintillation. The crest factor of the instantaneous signal with respect to its RMS value is typically of the order of 10 but it often reaches a level as high as 20 to 50. This requires an unusually wide dynamic range for the instruments, especially for the RMS meters which had to be operated at or below 25% of full scale. Consequently, relative errors of 10 to 15% are to be expected.

The proposed model must of course be applicable on the atmospheric scale. To verify this, we use the atmospheric data reprinted from Fig. 19 of Ref. 7 with permission of IEEE, Inc. As is always the case in field experiments, measurements were taken for different values of the similarity parameters η_o and b. However, both η_o and b are smaller than 0.01, as shown in Table I, and, thus, can be made equal to zero with no detectable errors on the solution for the normalized irradiance standard deviation β. The results are illustrated in Fig. 9. The agreement between theory and data is as good as can be throughout the propagation range. This is to be contrasted with recent models where the predicted β is too small in the strong scintillation region, e.g. Refs. 7 and 10.

The universality of the empirical constants C and γ cannot be established in all certainty but the results of Figs. 2 to 9 indicate that they are very likely universal. Differences by a factor of two in beam diameter are very well handled by the theory. However, the strongest test comes from the successful prediction of simulated and atmospheric data. Dimensionally, the all-important governing parameter C_n differs by a factor of about 500 and the propagation distances by about 300. These represent experimental conditions that are certainly as far apart as can be expected and the model works extremely well in both cases, as shown by Figs. 2 and 9.

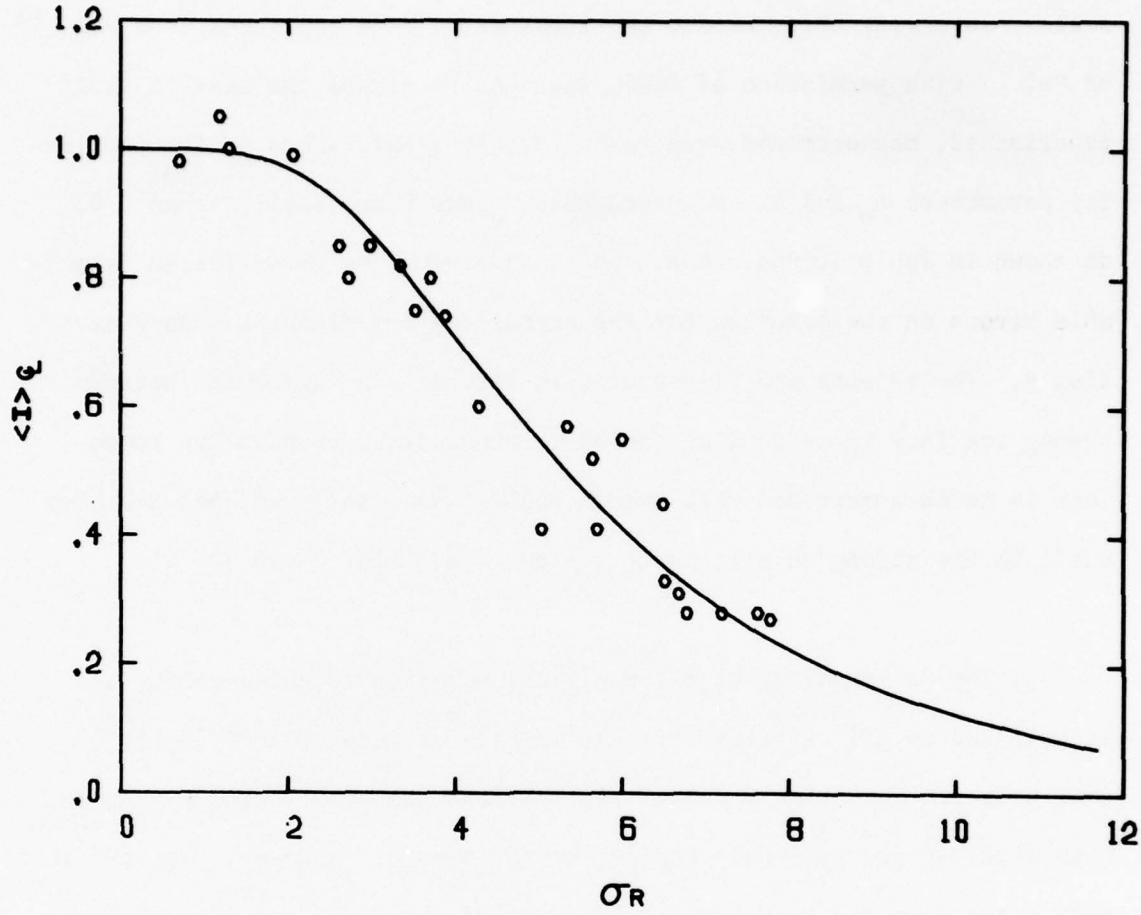

FIGURE 4 - The average irradiance measured on the axis of an 11 mm diam collimated laser beam plotted versus the Rytov formula for the log-irradiance standard deviation, σ_R. The experimental parameters are listed in Table I. The solid curve is the theoretical solution obtained with the method of this paper.

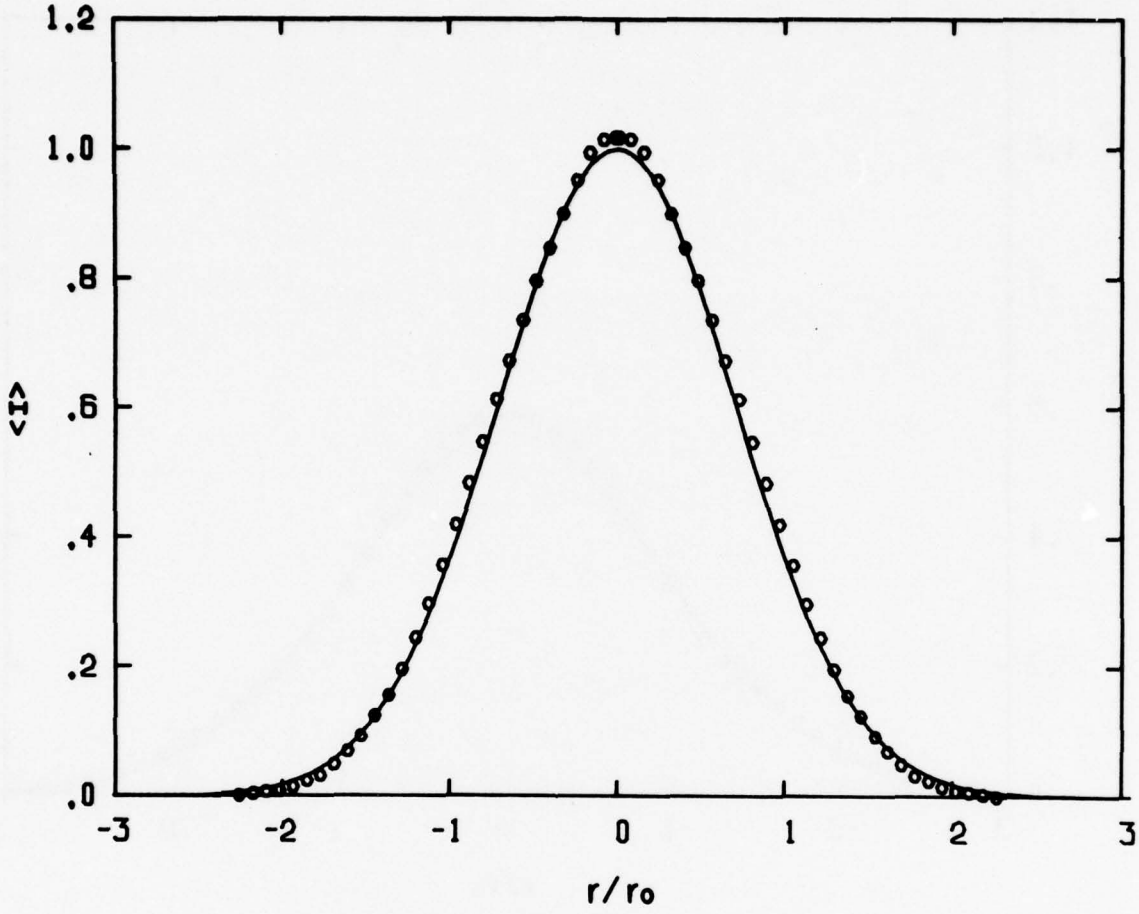

FIGURE 5 - The average irradiance profile of a 25 mm diam collimated laser beam measured at σ_R=1.2. The experimental parameters are listed in Table I. The solid curve is the theoretical solution obtained with the method of this paper.

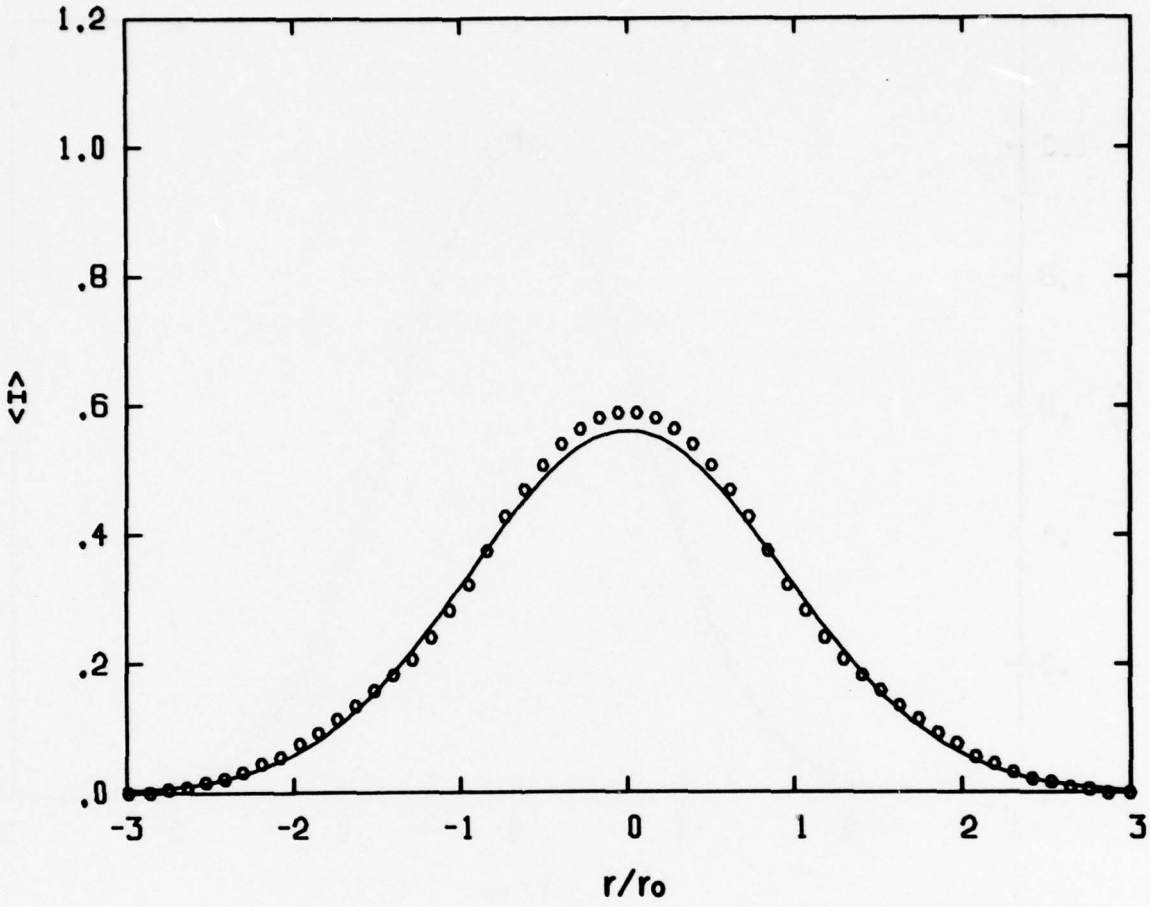

FIGURE 6 - The average irradiance profile of a 25 mm diam collimated laser beam measured at σ_R=8.5. The experimental parameters are listed in Table I. The solid curve is the theoretical solution obtained with the method of this paper.

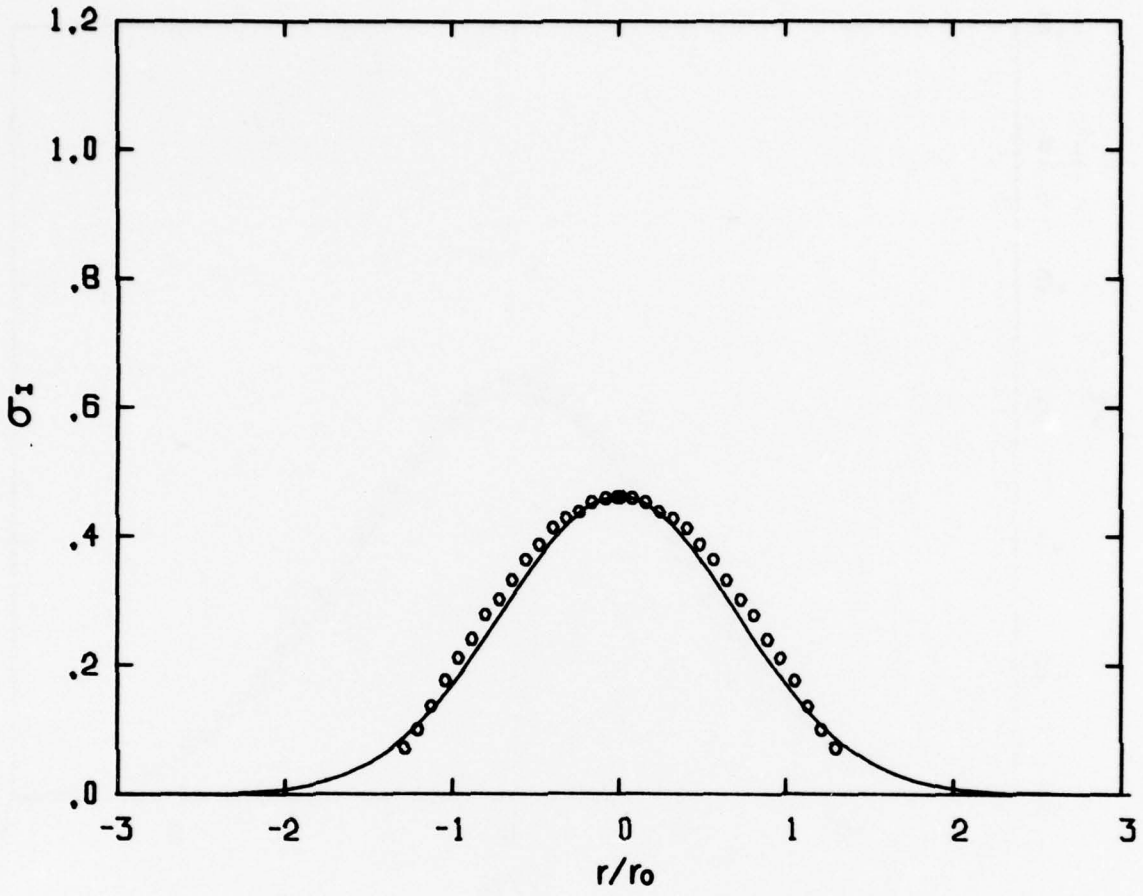

FIGURE 7 - The irradiance standard deviation profile of a 25 mm diam collimated laser beam measured at σ_R=1.2. The experimental parameters are listed in Table I. The solid curve is the theoretical solution obtained with the method of this paper.

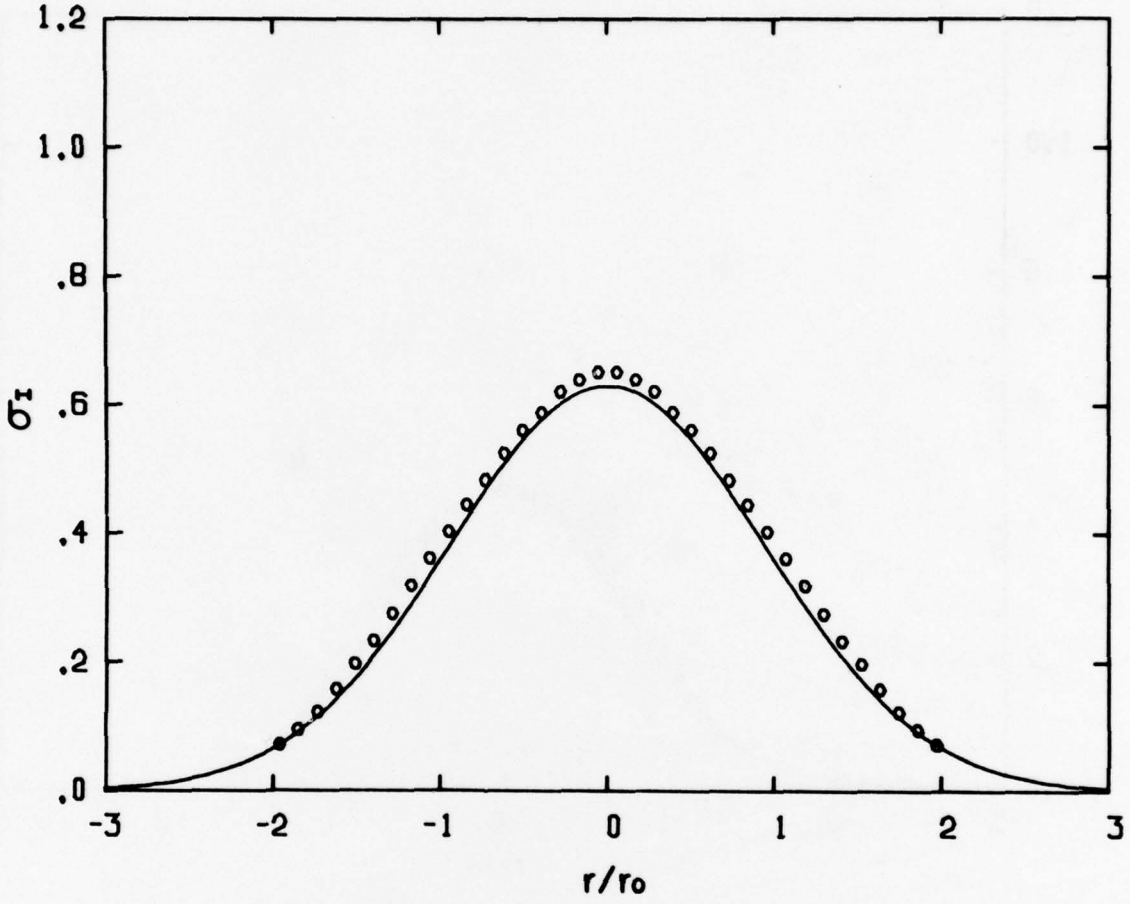

FIGURE 8 - The irradiance standard deviation profile of a 25 mm diam collimated laser beam measured at σ_R=8.5. The experimental parameters are listed in Table I. The solid curve is the theoretical solution obtained with the method of this paper.

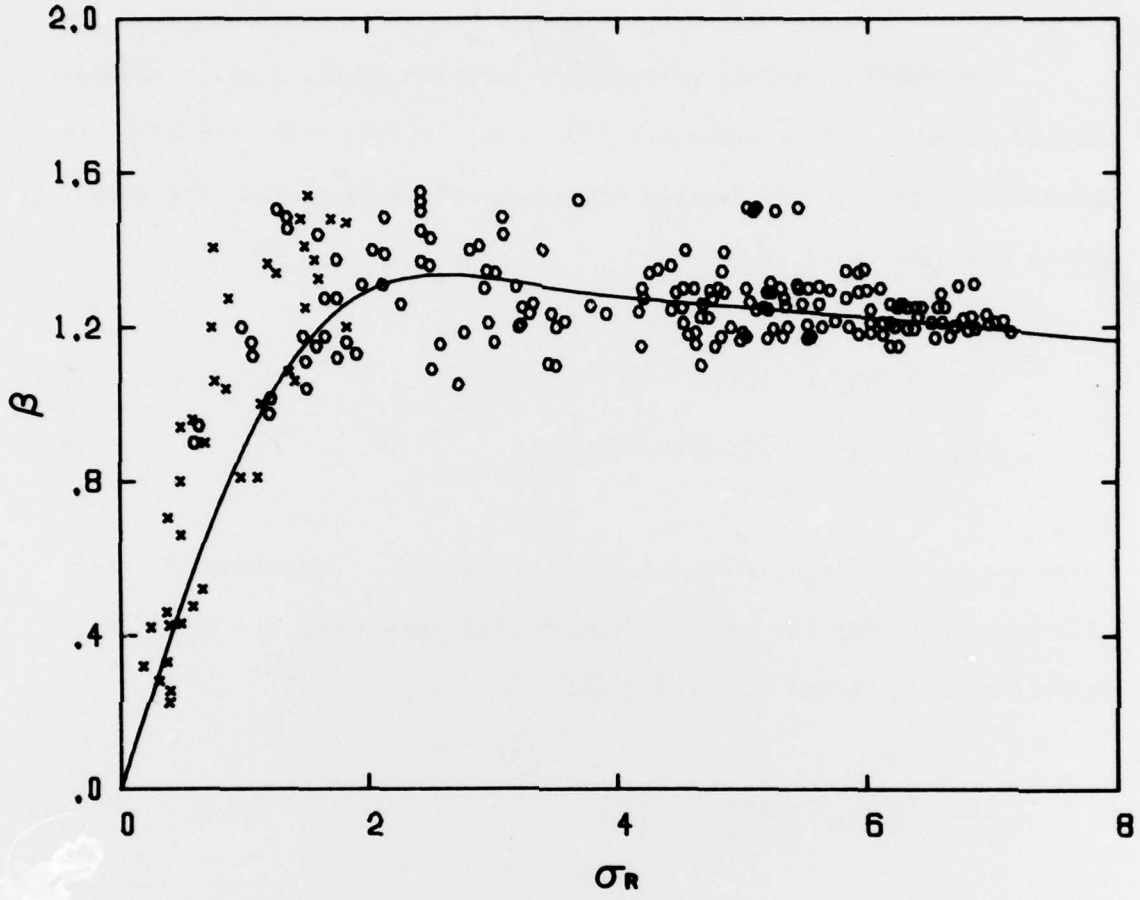

FIGURE 9 - The normalized irradiance standard deviation, $\beta=\sigma_I/\langle I\rangle$, measured in the atmosphere and reprinted from Fig. 19 of Ref. 7 with permission of IEEE, Inc. The experimental parameters are listed in Table I. The solid curve is the theoretical solution obtained with the method of this paper.

5.4 Discussion

The model equations predict a saturation level of unity independent of geometry. From equations (60), (61), (63b), (65), and (78), it is easy to show that the average amplitude and the amplitude variance behave asymptotically as:

$$\langle A \rangle \sim \exp\left[-.155\,\eta^{11/6}\right]\; H(\eta, \underset{\sim}{r}/r_o) \quad , \tag{80}$$

$$\langle aa \rangle \sim \exp\left[-.055\,\eta^{2}\right]\; G(\eta, \underset{\sim}{r}/r_o) \quad , \tag{81}$$

where H and G are regular functions of η and $\underset{\sim}{r}/r_o$. Equations (80) and (81) show that both $\langle A \rangle$ and $\langle aa \rangle$ vanish with increasing η. Therefore, we have from equations (12) and (74):

$$\lim_{\eta \to \infty} \frac{\sigma_I}{\langle I \rangle} = \frac{\langle aa^* \rangle}{\langle aa^* \rangle} = 1 \quad , \tag{82}$$

uniformly and independently of boundary conditions. This result is in good agreement with a recent theoretical treatment (Ref. 16) and seems to be confirmed by almost every set of experimental data. In particular, the predicted slow decay toward saturation as indicated by the small constant in the exponential of equation (81) agrees well with the experimental trend.

Supersaturation has a simple physical interpretation; it occurs because the real and imaginary parts of the fluctuating complex wave amplitude are statistically correlated and have unequal variances. A measure of this effect is given by the magnitude of the moment $\langle aa \rangle$ plotted against σ_R in Fig. 10 for the special case of a plane wave, b=0, with η_o=0. $|\langle aa \rangle|/\langle I \rangle$ rapidly increases from zero at $\sigma_R \approx 0$ to a maximum of about 0.85 at $\sigma_R \simeq 3$ and then slowly decreases back to zero asymptotically. That this behaviour is connected with supersaturation is clear from equation (74) which shows that $|\langle aa \rangle|^2$ contributes directly to σ_I^2.

The following simple example shows how correlation between the real and imaginary parts of the random amplitude can give rise to supersaturation of the normalized irradiance variance. Consider the fluctuating functions a_1 and a_2 given by:

$$a_1 = \sin \tau + i \sin \tau \quad , \tag{83}$$

$$a_2 = \sin \tau + i \cos \tau \quad , \tag{84}$$

where τ is a random variable uniformly distributed between 0 and 2π. The correlation factor between the real and imaginary parts of a_1 is one and it is zero for a_2. Assuming for simplicity that $\langle A_1 \rangle = \langle A_2 \rangle = 0$ and then calculating the normalized irradiance variances corresponding to a_1 and a_2, we find:

$$\frac{\langle a_1 a_1^* \; a_1 a_1^* \rangle}{\langle a_1 a_1^* \rangle^2} = \frac{\langle \sin^4 \tau \rangle}{\langle \sin^2 \tau \rangle^2} = \frac{3}{2} \quad , \tag{85}$$

$$\frac{\langle a_2 a_2^* \; a_2 a_2^* \rangle}{\langle a_2 a_2^* \rangle^2} = \frac{\langle \sin^4 \tau \rangle + \langle \cos^4 \tau \rangle + 2\langle \sin^2 \tau \cos^2 \tau \rangle}{\left[\langle \sin^2 \tau \rangle + \langle \cos^2 \tau \rangle\right]^2} = 1. \tag{86}$$

Therefore, the one case with nonzero correlation between the real and imaginary parts gives a larger normalized irradiance variance than the other case with zero correlation.

The excellent agreement between theory and data shown in Figs. 2 and 9 confirms the validity of the expressions (72) and (73) for the third- and fourth-order amplitude moments. These relations were derived from the hypothesis of normal probability distribution of the complex amplitude A defined in equation (1). Hence, measurements justify a posteriori the latter hypothesis for the purpose of relating irradiance variance to the first- and second-order amplitude moments, and this for the complete propagation range. Normal probability distribution for amplitude does not mean, as implied in Ref. 27, that the irradiance should follow a Rice-Nakagami or a Rayleigh distribution. Indeed, the latter distributions assume that the real and imaginary parts of the fluctuating amplitude have equal variances and are statistically uncorrelated. Should this be the case, the magnitude of $\langle aa \rangle$ would remain zero everywhere in contrast with the results of Fig. 10. Actually, this figure shows that the asymptotic limit of zero for $|\langle aa \rangle|$ becomes applicable only for $\sigma_R \gtrsim 20$.

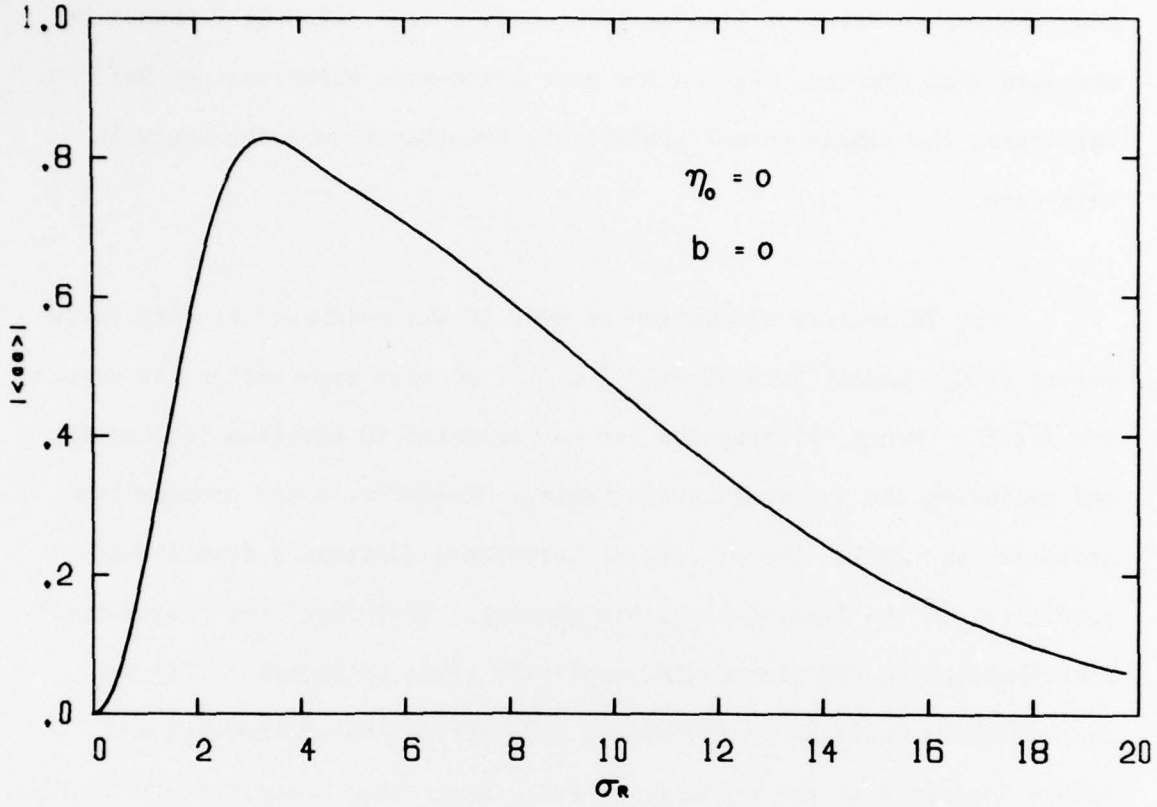

FIGURE 10 - The predicted magnitude of the second-order amplitude moment, $|\langle aa \rangle|$, for a plane wave, b=0, with η_o=0 plotted versus the Rytov formula for the log-irradiance standard deviation, σ_R.

Data from a recent simulation experiment (Ref. 30) show a supersaturation level as high as 1.7. Such a high value of β cannot be obtained from equation (74) in the near plane-wave experiment of Ref. 30. Therefore, the simple normal probability hypothesis does not apply in this case.

The laboratory simulation of Ref. 30 was conducted at very large values of C_n, namely 3 to 23.5×10^{-4} $m^{-1/3}$, so that supersaturation occurs for $\sqrt{\lambda z} < \ell_o$. Hence, diffraction can be neglected in equation (69) up to and including the supersaturation region. Moreover, since propagation distances are small, the effects of turbulence scattering from inhomogeneities off the line-of-sight are minimal. Therefore, the "log-normal" contributions to the fluctuating amplitude given by equation (71) are only slightly modified by turbulence and diffraction scatterings and become important in the vicinity of $z = 2z_A$ where the "normal" contributions, equation (70), begin to saturate because of fading of the coherent amplitude $\langle A \rangle$.

The log-normal expression for the normalized irradiance variance is given by (Ref. 31):

$$\beta^2 = \frac{\langle AA^* \rangle^2 \left| \langle A^2 \rangle \right|^2}{\left[\langle A \rangle \langle A \rangle^* \right]^4} - 1 \quad , \tag{87}$$

where $\left| \langle A^2 \rangle \right|$ denotes the magnitude of the complex quantity $\langle A^2 \rangle$. Equation (87) would replace (74) if the probability distribution were exactly

log-normal. This expression can give very large values of β owing to the presence of the vanishing average amplitude <A> in the denominator; actually, β would diverge to infinity if equation (87) were used for $z \gtrsim 2z_A$ (Ref. 31).

Since the experimental conditions of Ref. 30 imply an amplitude probability distribution in the supersaturation region closer to log-normal than is the case in the atmosphere or in Refs. 28 and 29, an expression combining (74) and (87) should be used instead of (74). This would give larger predicted values of β in accordance with measurements. However, as propagation distance increases with respect to ℓ_o, diffraction and turbulence scatterings become important and, with them, Gaussian statistics for the complex amplitude. Hence, even if β reaches a larger supersaturation level than in ordinary experiments, it should still saturate at a value of one, which is very well confirmed by the data of Ref. 30. Therefore, the qualitative model of amplitude probability distribution derived from equation (69) constitutes a plausible explanation for the unusually high supersaturation results of Ref. 30. These probability effects have no consequences on the model equations (60) to (65). However, the dependence on Prandtl number of the weak perturbation solutions derived in Ref. 30 means comparable changes in our functions $K(\eta)$, $R(\eta)$ and $T(\eta)$. This aspect will be studied in subsequent work.

6.0 CONCLUSION

A semi-empirical model of laser beam propagation in turbulence was developed. Solutions for average irradiance and irradiance variance profiles are very well confirmed by measurements over a wide range of turbulence conditions. Precision is better than with theories previously known.

The model is in the form of a closed set of simultaneous second-order partial differential equations for the amplitude moments. The equations, which are linear and contain only algebraic coefficients, are uniformly valid over the complete propagation range. Solutions are easily calculated for any beam geometry by straightforward finite difference techniques and they require very little computation time.

The algebraic coefficients were derived from simple approximations and contain two universal empirical constants. A full theoretical base could be worked out subject to new developments on the dependence of the phase and amplitude covariance functions on longitudinal separation. However, the excellent agreement between predictions and data shows that the approximate and empirical method used in this paper is very satisfactory for practical applications. The need for two empirical constants is well compensated for by the simplicity of the model.

7.0 ACKNOWLEDGMENTS

I am pleased to acknowledge the able technical assistance of A. Perreault, R. Rochette and J.-P. St-Hilaire. Data reduction and handling were made by P. Guay. I would also like to thank M. Gravel for support and help and N. Duchesne who showed skill and patience in typing this report, particularly the equations. The drawing of Fig. 1 is the work of R. Dubé.

REFERENCES

1. Tatarskii, V.I., "Wave Propagation in a Turbulent Medium", Dover Publication, New York, 1967.

2. Tatarskii, V.I., "The Effects of the Turbulent Atmosphere on Wave Propagation", National Technical Information Service, U.S. Dept. of Commerce, Springfield, Va., 1971, UNCLASSIFIED

3. De Wolf, D.A., "Saturation of Irradiance Fluctuations Due to Turbulent Atmosphere", J. Opt. Soc. Am., Vol. 58, No. 4, p. 461, 1968.

4. De Wolf, D.A., "Strong Irradiance Fluctuations in Turbulent Air: Plane Waves", J. Opt. Soc. Am., Vol. 63, No. 2, p. 171, 1973.

5. De Wolf, D.A., "Strong Irradiance fluctuations in turbulent air, II. Spherical waves", J. Opt. Soc. Am., Vol. 63, No. 10, p. 1249, 1973.

6. De Wolf, D.A., "Strong irradiance fluctuations in turbulent air, III. Diffraction cutoff", J. Opt. Soc. Am., Vol. 64, No. 3, p. 360, 1974.

7. Prokhorov, A.M., Bunkin, F.V., Gochelashvily, K.S. and Shishov, V.I., "Laser Irradiance Propagation in Turbulent Media", Proc. of the IEEE, Vol. 63, No. 5, p. 790, 1975.

8. Brown, W.P. Jr., "Fourth Moment of a Wave Propagating in a Random Medium", J. Opt. Soc. Am., Vol. 62, No. 8, p. 966, 1972.

9. Beran, J.J. and Whitman, A.M., "Free-space propagation of irradiance fluctuations and the fourth-order coherence function", J. Opt. Soc. Am., Vol. 64, No. 12, p. 1636, 1974.

10. Fante, R.F., "Irradiance scintillation: Comparison of theory with experiment", J. Opt. Soc. Am., Vol. 65, no. 5, p. 548, 1975.

11. Whitman, A.M. and Beran, M.J., "Asymptotic theory of irradiance fluctuations in a beam propagating in a random medium", J. Opt. Soc. Am., Vol. 65, No. 7, p. 765, 1975.

12. Lutomirski, R.F. and Yura, H.T., "Propagation of Finite Optical Beam in an Inhomogeneous Medium", Appl. Opt., Vol. 10, No. 7, p. 1652, 1971.

13. Yura, H.T., "Physical model for strong optical-amplitude fluctuations in a turbulent medium", J. Opt. Soc. Am., Vol. 64, No. 1, p. 59, 1974.

14. Clifford, S.F., Ochs, G.R. and Lawrence, R.S., "Saturation of optical scintillation by strong turbulence", J. Opt. Soc. Am., Vol. 64, No. 2, p. 148, 1974.

15. Banakh, V.A., Krekov, G.M., Mironov, V.L., Khmelevtsov, S.S. and Tsvik, R. Sh., "Focused-laser-beam scintillations in the turbulent atmosphere", J. Opt. Soc. Am., Vol. 64, No. 4, p. 516, 1974.

16. Lee, H.M., Elliot, R.A., Holmes, J.F. and Kerr, J.R., "Variance of irradiance for saturated scintillations", J. Opt. Soc. Am., Vol. 66, No. 12, p. 1389, 1976.

17. Dunphy, J.R. and Kerr, J.R., "Turbulence effects on target illumination by laser sources: phenomenolotical analysis and experimental results", Appl. Opt., Vol. 16, No. 5, p. 1345, 1977.

18. Sancer, M.I. and Varvatsis, A.D., "Saturation Calculation for Light Propagation in the Turbulent Atmosphere", J. Opt. Soc. Am., Vol. 60, No. 5, p. 654, 1970.

19. Brown, W.P. Jr., "Calculation of the Variance of Irradiance Scintillation", J. Opt. Soc. Am., Vol. 61, No. 7, p. 981, 1971.

20. Bissonnette, L.R., "A Semi-Empirical Closure Theory of Optical and IR Wave Propagation in Turbulent Media", DREV R-708/74, September 1974, UNCLASSIFIED

21. Born, M. and Wolf, E., "Principles of Optics", Pergamon Press, 4th edition, 1970.

22. Batchelor, G.K., "The Theory of Homogeneous Turbulence", Cambridge University Press, Cambridge, 1960.

23. Bradshaw, P., editor, "Turbulence", Topics in Applied Physics, Vol. 12, Springer-Verlag, New York, 1976.

24. Strohbehn, J.W., "Line-of-Sight Propagation Through the Turbulent Atmosphere", Proc. of the IEEE, Vol. 56, No. 8, p. 1301, 1968.

25. Lawrence, R.S. and Strohbehn, J.W., "A Survey of Clear-Air Propagation Effects Relevant to Optical Communications", Proc. of the IEEE, Vol. 58, No. 10, p. 1523, 1970.

26. Yura, H.T., "Physical Model for Strong Optical Wave Fluctuations in the Atmosphere", AGARD Conference Proceedings No. 183 on Optical Propagation in the Atmosphere, Defence Scientific Information Service, Ottawa, 1975, UNCLASSIFIED

27. Strohbehn, J.W., Wang, T-i and Speck, J.P., "On the probability distribution of line-of-sight fluctuations of optical signals", Radio Science, Vol. 10, No. 1, p. 59, 1975.

28. Bissonnette, L.R., "Atmospheric scintillation of optical and infrared waves: a laboratory simulation", Appl. Opt., Vol. 16, No. 8, p. 2242, 1977.

29. Bissonnette, L.R., "Laboratory Simulation of Atmospheric Turbulence for Optical Propagation Studies", DREV Report 4075/77, August 1977, UNCLASSIFIED

30. Gurvich, A.S., Kallistratova, M.A. and Martvel', F.E., "Investigation of Strong Fluctuations of the Light Intensity in a Turbulent Medium at a Small Wave Parameter", Radiophysics, Vol. 20, No. 7, p. 1020, 1977, (in Russian).

31. Bissonnette, L.R., "Probability Distribution and Asymptotic Variance of Strong Irradiance Fluctuations of Optical Waves in Turbulent Media", DREV Report 4042/75, October 1975, UNCLASSIFIED

CRDV R-4104/78 (UNCLASSIFIED)

Bureau - Recherche et Développement, Ministère de la Défense nationale, Canada.
CRDV, C.P. 880, Courcelette, Que. G0A 1R0.

"Average Irradiance and Irradiance Variance of Laser Beams in Turbulent Media"
by L.R. Bissonnette

On a mis au point un modèle semi-empirique de la propagation de faisceau laser en milieux turbulents sous la forme d'un système fermé d'équations aux dérivées partielles du second ordre pour les moments statistiques du premier et du second ordres de l'amplitude de l'onde lumineuse. Ces équations sont linéaires, ne contiennent que des coefficients algébriques et sont uniformément valides à toutes les distances de propagation. On montre que l'hypothèse de la fonction de probabilité normale de l'amplitude complexe de l'onde est compatible avec l'équation d'onde stochastique. Cette hypothèse est utilisée pour écrire la variance de l'intensité en fonction des moments d'ordres un et deux de l'amplitude. Les profils de l'intensité moyenne et de la variance de l'intensité des faisceaux laser sont facilement et rapidement calculés au moyen d'une méthode numérique aux différences finies. Les résultats sont en excellent accord avec des mesures expérimentales prises dans l'atmosphère et en milieu de simulation. (NC)

CRDV R-4104/78 (UNCLASSIFIED)

Bureau - Recherche et Développement, Ministère de la Défense nationale, Canada.
CRDV, C.P. 880, Courcelette, Que. G0A 1R0.

"Average Irradiance and Irradiance Variance of Laser Beams in Turbulent Media"
by L.R. Bissonnette

On a mis au point un modèle semi-empirique de la propagation de faisceau laser en milieux turbulents sous la forme d'un système fermé d'équations aux dérivées partielles du second ordre pour les moments statistiques du premier et du second ordres de l'amplitude de l'onde lumineuse. Ces équations sont linéaires, ne contiennent que des coefficients algébriques et sont uniformément valides à toutes les distances de propagation. On montre que l'hypothèse de la fonction de probabilité normale de l'amplitude complexe de l'onde est compatible avec l'équation d'onde stochastique. Cette hypothèse est utilisée pour écrire la variance de l'intensité en fonction des moments d'ordres un et deux de l'amplitude. Les profils de l'intensité moyenne et de la variance de l'intensité des faisceaux laser sont facilement et rapidement calculés au moyen d'une méthode numérique aux différences finies. Les résultats sont en excellent accord avec des mesures expérimentales prises dans l'atmosphère et en milieu de simulation. (NC)

CRDV R-4104/78 (UNCLASSIFIED)

Bureau - Recherche et Développement, Ministère de la Défense nationale, Canada.
CRDV, C.P. 880, Courcelette, Que. G0A 1R0.

"Average Irradiance and Irradiance Variance of Laser Beams in Turbulent Media"
by L.R. Bissonnette

On a mis au point un modèle semi-empirique de la propagation de faisceau laser en milieux turbulents sous la forme d'un système fermé d'équations aux dérivées partielles du second ordre pour les moments statistiques du premier et du second ordres de l'amplitude de l'onde lumineuse. Ces équations sont linéaires, ne contiennent que des coefficients algébriques et sont uniformément valides à toutes les distances de propagation. On montre que l'hypothèse de la fonction de probabilité normale de l'amplitude complexe de l'onde est compatible avec l'équation d'onde stochastique. Cette hypothèse est utilisée pour écrire la variance de l'intensité en fonction des moments d'ordres un et deux de l'amplitude. Les profils de l'intensité moyenne et de la variance de l'intensité des faisceaux laser sont facilement et rapidement calculés au moyen d'une méthode numérique aux différences finies. Les résultats sont en excellent accord avec des mesures expérimentales prises dans l'atmosphère et en milieu de simulation. (NC)

CRDV R-4104/78 (UNCLASSIFIED)

Bureau - Recherche et Développement, Ministère de la Défense nationale, Canada.
CRDV, C.P. 880, Courcelette, Que. G0A 1R0.

"Average Irradiance and Irradiance Variance of Laser Beams in Turbulent Media"
by L.R. Bissonnette

On a mis au point un modèle semi-empirique de la propagation de faisceau laser en milieux turbulents sous la forme d'un système fermé d'équations aux dérivées partielles du second ordre pour les moments statistiques du premier et du second ordres de l'amplitude de l'onde lumineuse. Ces équations sont linéaires, ne contiennent que des coefficients algébriques et sont uniformément valides à toutes les distances de propagation. On montre que l'hypothèse de la fonction de probabilité normale de l'amplitude complexe de l'onde est compatible avec l'équation d'onde stochastique. Cette hypothèse est utilisée pour écrire la variance de l'intensité en fonction des moments d'ordres un et deux de l'amplitude. Les profils de l'intensité moyenne et de la variance de l'intensité des faisceaux laser sont facilement et rapidement calculés au moyen d'une méthode numérique aux différences finies. Les résultats sont en excellent accord avec des mesures expérimentales prises dans l'atmosphère et en milieu de simulation. (NC)

DREV R-4104/78 (UNCLASSIFIED)

Research and Development Branch, Department of National Defence, Canada.
DREV, P.O. Box 880, Courcelette, Que. G0A 1R0.

"Average Irradiance and Irradiance Variance of Laser Beams in Turbulent Media"
by L.R. Bissonnette

A semi-empirical model of laser beam propagation in turbulence is written in the form of a closed set of second-order partial differential equations for the first- and second-order amplitude moments. The equations are linear, contain only algebraic coefficients, and are uniformly valid over the complete propagation range. The hypothesis of normal probability distribution of the complex wave amplitude is shown to be consistent with the stochastic wave equation, and is used to obtain the irradiance variance in terms of the first- and second-order amplitude moments. Solutions for average irradiance and irradiance variance profiles of laser beams are easily and quickly calculated by a mumerical finite difference method. Predictions agree very well with experimental data in the atmosphere and in a simulation medium. (U)

DREV R-4104/78 (UNCLASSIFIED)

Research and Development Branch, Department of National Defence, Canada.
DREV, P.O. Box 880, Courcelette, Que. G0A 1R0.

"Average Irradiance and Irradiance Variance of Laser Beams in Turbulent Media"
by L.R. Bissonnette

A semi-empirical model of laser beam propagation in turbulence is written in the form of a closed set of second-order partial differential equations for the first- and second-order amplitude moments. The equations are linear, contain only algebraic coefficients, and are uniformly valid over the complete propagation range. The hypothesis of normal probability distribution of the complex wave amplitude is shown to be consistent with the stochastic wave equation, and is used to obtain the irradiance variance in terms of the first- and second-order amplitude moments. Solutions for average irradiance and irradiance variance profiles of laser beams are easily and quickly calculated by a mumerical finite difference method. Predictions agree very well with experimental data in the atmosphere and in a simulation medium. (U)

DREV R-4104/78 (UNCLASSIFIED)

Research and Development Branch, Department of National Defence, Canada.
DREV, P.O. Box 880, Courcelette, Que. G0A 1R0.

"Average Irradiance and Irradiance Variance of Laser Beams in Turbulent Media"
by L.R. Bissonnette

A semi-empirical model of laser beam propagation in turbulence is written in the form of a closed set of second-order partial differential equations for the first- and second-order amplitude moments. The equations are linear, contain only algebraic coefficients, and are uniformly valid over the complete propagation range. The hypothesis of normal probability distribution of the complex wave amplitude is shown to be consistent with the stochastic wave equation, and is used to obtain the irradiance variance in terms of the first- and second-order amplitude moments. Solutions for average irradiance and irradiance variance profiles of laser beams are easily and quickly calculated by a mumerical finite difference method. Predictions agree very well with experimental data in the atmosphere and in a simulation medium. (U)

DREV R-4104/78 (UNCLASSIFIED)

Research and Development Branch, Department of National Defence, Canada.
DREV, P.O. Box 880, Courcelette, Que. G0A 1R0.

"Average Irradiance and Irradiance Variance of Laser Beams in Turbulent Media"
by L.R. Bissonnette

A semi-empirical model of laser beam propagation in turbulence is written in the form of a closed set of second-order partial differential equations for the first- and second-order amplitude moments. The equations are linear, contain only algebraic coefficients, and are uniformly valid over the complete propagation range. The hypothesis of normal probability distribution of the complex wave amplitude is shown to be consistent with the stochastic wave equation, and is used to obtain the irradiance variance in terms of the first- and second-order amplitude moments. Solutions for average irradiance and irradiance variance profiles of laser beams are easily and quickly calculated by a mumerical finite difference method. Predictions agree very well with experimental data in the atmosphere and in a simulation medium. (U)